Bond lengths and coordination numbers from $L_{2,3}$-edge versus K-edge surface extended x-ray-absorption fine structure

P. H. Citrin
AT&T Bell Laboratories, Murray Hill, New Jersey 07974
(Received 26 July 1984)

The interference between final states of s and d symmetry arising from anisotropic $L_{2,3}$-edge absorption is explicitly considered. Previous arguments by others that such an interference can significantly affect the amplitude and phase of the $L_{2,3}$-edge surface extended x-ray-absorption fine structure (SEXAFS) had been based on calculated phase shifts and analysis of simulated data. Here, empirical methods are developed to isolate the effects of the interference. For the case of $L_{2,3}$-edge absorption from iodine it is shown that the calculated s- and d-state phase-shift differences are about a factor of 2 larger than the experimental value. This result accounts for the success of earlier $L_{2,3}$-edge SEXAFS amplitude analyses which approximate the interference by simple addition of the d and coupled s-d absorption terms. The previously argued effect on the SEXAFS phase correction is also shown to be too large by about a factor of 2 as a result of the analysis procedure used in that work. The effects of the interference are explored as a function of absorbing adatom, adsorption site, and accuracy of the calculated s and d-state phase-shift differences. With the assumption that these calculated values are reliable it is shown that only the atop configuration should manifest a measurable phase correction (corresponding to ~ 0.01 Å in the bond length) and that the additive approximation used in the earlier SEXAFS studies of I and Te should be valid for all atoms. In the absence of data from other elements to test the accuracy of the calculated phase shifts, a general and theory-independent procedure was developed for analyzing $L_{2,3}$-edge data. This procedure removes the effects of the interference and allows bond lengths and adsorption sites to be determined with a reliability comparable to that obtained from K-edge SEXAFS data.

I. INTRODUCTION

Analysis of the frequency and amplitude of the extended x-ray-absorption fine structure[1] (EXAFS) from atoms in even complex bulk systems has been shown[2–8] to provide reliable structural information directly in terms of bond lengths and coordination numbers around the absorbing atom. The application of EXAFS to atoms adsorbed on the surface of single crystals[9–11] (SEXAFS) provides additional information about their spatial orientation with respect to the substrate atoms because the photoabsorption cross section, usually isotropic in most materials,[12] is anisotropic for the adatoms. Varying the direction of x-ray polarization with respect to the adsorbate-substrate bond(s) thus changes the SEXAFS amplitude, and this information can be used to complement the determination of adsorption-site geometries.[11,13–18]

For $L_{2,3}$-edge absorption, the polarization dependence of the SEXAFS amplitude is more complicated than that for K-edge absorption. The reason for this is that the photoabsorption probability for initial s states (e.g., K or L_1 edges) involves final states of only p symmetry, whereas that of L_2 or L_3 edges involves final states of both s and d symmetry whose coupled strength is nonzero for anisotropic absorbers.[19,20] Neglect of this s-d cross term for such absorbers can affect not only the determination of their coordination number (adsorption-site geometry), but also their bond lengths. Approximate modifications to the analysis of SEXAFS amplitudes from $L_{2,3}$ edges as a result of this cross term have been mentioned previously,[11(b)] but only the results of corrections applied to the analysis of SEXAFS bond lengths were reported in recent abbreviated work.[14,15] An account of these bond-length corrections was not presented because, as will be shown in this work, for all but one adsorption geometry the corrections are negligible ($\lesssim 0.01$ Å), and even for this exceptional case the corrections can be completely eliminated.

Recently, however, Stöhr and Jaeger[21] (SJ) considered the effects of the s-d cross term and concluded that neglect of the cross term or approximate modifications in the analysis of $L_{2,3}$-edge SEXAFS data can lead not only to significant errors in the derived bond length, but also to erroneous assignments of the chemisorption site. Such conclusions, if correct, would have important implications on the analysis of SEXAFS data and the ability of that technique to obtain reliable adsorption geometries.

In this work the differences between K- and $L_{2,3}$-edge SEXAFS data are explicitly considered. A method of analysis is presented which allows such differences to be removed in the determination of bond lengths and coordination numbers from anisotropic $L_{2,3}$-edge absorption spectra. The conclusions of SJ are examined and corrected. General implications of the effect of the s-d cross term in $L_{2,3}$-edge SEXAFS measurements are also discussed.

II. BACKGROUND

A. K edges

The usual expression for the SEXAFS $\chi(k)$ from a K or L_1 edge of an atom surrounded by N nearest neighbors at a single distance R is given by[22]

$$\chi(k,\theta)\approx A'(k)N_S(\theta)\sin[2kR+\phi_{1b}(k)] , \quad K \text{ or } L_1 \text{ edges} . \tag{1}$$

Here k is the photoelectron momentum defined as $[2m(E-E_0)^{1/2}/\hbar]$, where E is the photon energy and E_0 is the energy threshold of the absorption edge, and $\phi_{1b}(k)$ is the total phase shift experienced by the photoelectron. It is given by

$$\phi_{1b}(k)=\phi_a^{l=1}(k)+\phi_b(k)-\pi , \tag{2}$$

where ϕ_b is the backscattering phase shift due to the neutral neighbor and $\phi_a^{l=1}$ is twice the $l=1$ partial phase shift due to the outgoing and return scattering from the core-ionized absorbing atom. [The factor of π is included to preserve the correct overall sign of $\chi(k,\theta)$.]

Multiplying the SEXAFS sinusoid is the total amplitude function $A'(k)N_S(\theta)$. The first part of this function can be written as

$$A'(k)=f(\pi,k)(kR^2)^{-1}e^{-2k^2\sigma^2}e^{-2R/\lambda(k)} , \tag{3}$$

where $f(\pi,k)$ is the backscattering amplitude, $e^{-2k^2\sigma^2}$ is a Debye-Waller–type term containing a mean-square displacement σ, and $e^{-2R/\lambda(k)}$ is an inelastic scattering term containing an effective photoelectron mean free path λ. These terms (which, along with the R^{-2} factor, determine the short-range nature of the overall EXAFS amplitude) ordinarily do not affect the determination of R or the coordination number and will not be discussed further.[23] The second part of the total amplitude function is given by

$$N_S(\theta)=\sum_{i=1}^{N} 3\,|\,\hat{\epsilon}\cdot\hat{r}_i\,|^2, \quad K \text{ or } L_1 \text{ edges} . \tag{4}$$

$\hat{\epsilon}$ is the polarization of the x-ray photon and $\hat{r}_i$ is the unit vector connecting the absorbing atom and the ith neighboring atom in the coordination shell. For isotropically distributed atoms the quantity $N_S(\theta)$ averages to N, but for anisotropic absorbers it can range between 0 and $3N$. For this reason $N_S(\theta)$ is referred to as an *effective* surface coordination number.[9]

Comparison between the ratio of $N_S(\theta)$ measured at different values of θ (the angle between $\hat{\epsilon}$ and the surface normal) and that ratio calculated for adsorbate atoms occupying one of several possible surface geometries facilitates the empirical identification of the adsorption-site geometry [the ratio $N_S(\theta_1)/N_S(\theta_2)$ is called a *relative* amplitude[9]]. *Absolute* amplitudes can be obtained by normalizing the total amplitude of the unknown surface system $N_S(\theta)A'(k)$ to that of a structurally known model compound $N_M A'_M(k)$ containing the same absorbing and scattering atoms. The model compound is usually a powder or gas so N_M corresponds to a true (i.e., angularly averaged) coordination number. The bond length can be obtained by subtracting the argument of the model-compound EXAFS sinusoid, $2kR_M+\phi_{1b}(k)$, from that of the unknown system. Because the phase shifts are independent of chemical environment they cancel (phase-shift transferability[24]), leading to a very accurate determination of R. Further details of EXAFS data-analysis procedures can be found in Ref. 8 and references therein.

B. $L_{2,3}$-edges

The corresponding expression for the SEXAFS from the L_2 or L_3 edge of the same absorbing atom considered in Eq. (1) is given by[19,20,22]

$$\chi(k,\theta)\approx A'(k)\sum_{i=1}^{N}\{\tfrac{1}{2}(1+3\,|\,\hat{\epsilon}\cdot\hat{r}_i\,|^2)\,|\,M_{21}\,|^2\sin[2kR+\phi_{2b}(k)]+\tfrac{1}{2}\,|\,M_{01}^2\,|\sin[2kR+\phi_{0b}(k)]$$
$$+M_{01}M_{21}(1-3\,|\,\hat{\epsilon}\cdot\hat{r}_i\,|^2)\sin[2kR+\phi_{02b}(k)]\}(\,|\,M_{21}\,|^2+\tfrac{1}{2}\,|\,M_{01}\,|^2)^{-1} . \tag{5}$$

The three terms in curly brackets correspond to final states of pure d, pure s, and coupled s and d symmetries, respectively. The phase shifts are given by

$$\phi_{2b}(k)=\phi_a^{l=2}(k)+\phi_b(k) , \tag{6}$$

$$\phi_{0b}(k)=\phi_a^{l=0}(k)+\phi_b(k) , \tag{7}$$

$$\phi_{02b}(k)=\tfrac{1}{2}[\phi_a^{l=2}(k)+\phi_a^{l=0}(k)]+\phi_b(k) . \tag{8}$$

For convenience later on, Eq. (8) is rewritten as

$$\phi_{02b}(k)=\phi_{2b}(k)+\Delta_a(k) , \tag{9}$$

where

$$\Delta_a(k)=\tfrac{1}{2}[\phi_a^{l=0}(k)-\phi_a^{l=2}(k)] . \tag{10}$$

$\Delta_a(k)$ is the cross-term correction to the absorbing atom phase shift for purely d final-state scattering. The radial dipole matrix elements M_{01} and M_{21} couple the initial $2p$ ($l=1$) atomic wave function with the $l=2$ and 0 final states. Defining the ratio

$$c=M_{01}/M_{21} , \tag{11}$$

Eq. (5) may also be rewritten as

$$\chi(k,\theta)=A'(k)\{n_d(\theta)\sin[2kR+\phi_{2b}(k)]+n_s\sin[2kR+\phi_{0b}(k)]+n_{sd}(\theta)\sin[2kR+\phi_{2b}(k)+\Delta_a(k)]\} , \tag{12}$$

where

$$n_d(\theta)=0.5\left[\frac{2}{2+c^2}\right]\sum_{i=1}^{N}(1+3\,|\,\hat{\epsilon}\cdot\hat{r}_i\,|^2)\,, \tag{13}$$

$$n_s=0.5\left[\frac{c^2}{2+c^2}\right], \tag{14}$$

$$n_{sd}(\theta)=\left[\frac{2c}{2+c^2}\right]\sum_{i=1}^{N}(1-3\,|\,\hat{\epsilon}\cdot\hat{r}_i\,|^2)\,. \tag{15}$$

The quantities $n_d(\theta)$, n_s, and $n_{sd}(\theta)$ can be thought of as effective *partial* coordination numbers, although a completely physical analogy is absent since $n_{sd}(\theta)$ can take on negative values. The ratio c has been calculated[25] for a variety of elements and is found to be approximately 0.2 for $Z\gtrsim 20$ and relatively independent of k.[26] Substituting $c=0.2$ into Eqs. (13)–(15) and assuming $\frac{1}{2}c^2\approx 0$ gives the essentially exact and more simple expression

$$\chi(k,\theta)\approx A'(k)\{n_d(\theta)\sin[2kR+\phi_{2b}(k)] +n_{sd}(\theta)\sin[2kR+\phi_{2b}(k)+\Delta_a(k)]\}\,, \tag{16}$$

with

$$n_d(\theta)\approx 0.5\sum_{i=1}^{N}(1+3\,|\,\hat{\epsilon}\cdot\hat{r}_i\,|^2)\,, \tag{17}$$

$$n_{sd}(\theta)\approx 0.2\sum_{i=1}^{N}(1-3\,|\,\hat{\epsilon}\cdot\hat{r}_i\,|^2)\,. \tag{18}$$

For isotropic absorbers the *total s-d* cross term, i.e., the term multiplied by $n_{sd}(\theta)$ in Eq. (16), vanishes by angular averaging. For anisotropic absorbers this term will clearly affect both the determination of bond lengths and effective coordination numbers, but it is not at all clear by inspection how large the effects of that term will be.

1. $\Delta_a(k)=0$

The simplest way to account for the total cross term is to assume that, to first order, the effect of $\Delta_a(k)$ is negligible, i.e., the cross term modifies only the amplitude.[11(b)] Equation (16) can then be written as[27]

$$\chi(k,\theta)\approx A'(k)N_S(\theta)\sin[2kR+\phi_{2b}(k)]\,, \tag{19}$$

where here

$$N_S(\theta)=n_d(\theta)+n_{sd}(\theta) =\sum_{i=1}^{N}(0.7+0.9\,|\,\hat{\epsilon}\cdot\hat{r}_i\,|^2),\quad \Delta_a(k)=0\,. \tag{20}$$

This expression is of the same form as Eq. (1) for K edges and thus allows for the same analytical treatment of $L_{2,3}$-edge data.[11,14,15] The effect of including the approximate total cross term with $\Delta_a(k)=0$ also makes $N_S(\theta)$ for $L_{2,3}$ absorption even more isotropic, i.e., $\sum_i(0.7+0.9\,|\,\hat{\epsilon}\cdot\hat{r}_i\,|^2)$ in Eq. (20) versus $\sum_i(0.5+1.5\,|\,\hat{\epsilon}\cdot\hat{r}_i\,|^2)$ in Eq. (17). This is particularly so for the case of onefold atop adsorption because the relative fraction of the numerical constant (0.7 or 0.5) to the θ-dependent term is largest when $N=1$.

The fact that $L_{2,3}$-edge SEXAFS is always more isotropic than K-edge SEXAFS, even for atoms in high-symmetry adsorption sites, makes it clear why relative amplitudes from $L_{2,3}$-edge SEXAFS data alone are usually insufficient for a reliable determination of adsorption sites. Additional measurement of absolute amplitudes using model systems (or comparison with simulated data, discussed later on) and/or measurement of higher nearest-neighbor substrate distances are essential for unambiguous adsorption-site assignments.[28] This point has been emphasized previously[9,11,14,15] and will be seen to be important in the Discussion section below.

2. $\Delta_a(k)\neq 0$

The assumption in Eq. (19) that $\Delta_a(k)=0$ is only a simplifying approximation. Rewriting Eq. (16) for any value of $\Delta_a(k)$ gives the general expression

$$[A'(k)]^{-1}\chi(k,\theta)=\mathrm{Im}(n_d(\theta)\exp\{i[2kR+\phi_{2b}(k)]\}+n_{sd}(\theta)\exp\{i[2kR+\phi_{2b}(k)+\Delta_a(k)]\}) =\mathrm{Im}(n_d(\theta)\exp\{i[2kR+\phi_{2b}(k)]\}[\alpha(k,\theta)e^{i\psi(k,\theta)}])\,, \tag{21}$$

where

$$\alpha(k,\theta)=(\{1+[n_{sd}(\theta)/n_d(\theta)]\cos\Delta_a(k)\}^2 +[n_{sd}(\theta)/n_d(\theta)]^2\sin^2\Delta_a(k))^{1/2}\,. \tag{22}$$

and

$$\psi(k,\theta)=\tan^{-1}\left[\frac{[n_{sd}(\theta)/n_d(\theta)]\sin\Delta_a(k)}{1+[n_{sd}(\theta)/n_d(\theta)]\cos\Delta_a(k)}\right]. \tag{23}$$

Equations (21)–(23) allow the effect of the total cross term in Eq. (16), now incorporated into the term $\alpha(k,\theta)e^{i\psi(k,\theta)}$, to be seen in a straightforward way. Rewriting Eq. (16) for $L_{2,3}$ edges in the same form as Eq. (1) for K edges gives

$$\chi(k,\theta)=A'(k)N_S(\theta)\sin[2kR+\phi_{2b}(k)+\psi(k,\theta)]\,, \qquad L_{2,3}\text{ edges} \tag{24}$$

where now, in general,

$$N_S(\theta)=n_d(\theta)\alpha(k,\theta)\,. \tag{25}$$

For $L_{2,3}$-edge absorption, the total SEXAFS amplitude is

TABLE I. Expressions of $[A'(k)]^{-1}\chi(k)$ for $L_{2,3}$-edge absorption.

	Exact[a]	Approximate
Isotropic absorption	$n_d(\theta)\sin[2kR+\phi_{2b}(k)]$	$n_d(\theta)\sin[2kR+\phi_{2b}(k)]$
Anisotropic absorption	$n_d(\theta)\sin[2kR+\phi_{2b}(k)]$ $+n_{sd}(\theta)\sin[2kR+\phi_{2b}(k)+\Delta_a(k)]$	$[n_d(\theta)+n_{sd}(\theta)]\sin[2kR+\phi_{2b}(k)]$

[a]For $c\approx 0.2$ (see text) the normalization factor $2/(2+c^2)$ that multiplies n_d is ≈ 1 and the term $[c^2/(2+c^2)]\sin[2kR+\phi_{0b}(k)]$ is ≈ 0.

modified from $A'(k)n_d(\theta)$ (in the absence of the cross term) to $A'(k)n_d(\theta)\alpha(k,\theta)$, and the total SEXAFS phase is modified from $[2kR+\phi_{2b}(k)]$ to $[2kR+\phi_{2b}(k)+\psi(k,\theta)]$. If $\Delta_a(k)=0$, then $\psi(k,\theta)=0$ and $N_S(\theta)=n_d(\theta)+n_{sd}(\theta)$, i.e., the approximations of Eqs. (19) and (20) are obtained. The various conditions for $L_{2,3}$-edge absorption are summarized in Table I.

C. The problem

When $\Delta_a(k)$ is finite, there are variety of possible effects on the SEXAFS amplitude and phase which are, it will be seen, strongly dependent upon the sign and magnitude of $\Delta_a(k)$. One way to illustrate this dependence is to plot the real and imaginary parts of $\alpha(k,\theta)e^{i\psi(k,\theta)}$ for several different conditions of $\Delta_a(k)$, see Fig. 1. As stated above, the geometry most sensitive to these effects is the case of atop adsorption. It has been previously shown[14] that at saturation coverages I occupies the atop site on Si(111), so this particular system will be considered here as exemplary.[29] For the atop geometry $N=1$, and from Eqs. (17) and (18), $n_d(\theta)=0.5+1.5\cos^2\theta$ and $n_{sd}(\theta)=0.2-0.6\cos^2\theta$. The largest difference in the sign and magnitude of the individual $n_{sd}(\theta)$ and $n_d(\theta)$ terms and of their ratio is obtained when the polarization $\hat{\epsilon}$ is parallel versus perpendicular to the adsorbate-substrate bond lying along the surface normal, i.e., when $\theta=90°$ versus $\theta=0°$, respectively. Explicitly, $n_{sd}(90°)/n_d(90°)=0.2/0.5=0.4$, and $n_{sd}(0°)/n_d(0°)=-0.4/2.0=-0.2$. These ratios, extending from the point labeled 1 along the Re axis, are indicated by *light* dashed (0°) and dotted-dashed (90°) lines in Fig. 1(a) for the special case of $\Delta_I(k)=0$. Bold vertical fiducial marks along the Re axis are also indicated for this special condition, with the $\theta=90°$ mark being larger. The quantity $\alpha(k,\theta)$ is shown by *bold* dashed or dotted-dashed lines for the two different values of θ. These lines, extending from the origin to the respective fiducial mark, lie along the Re axis but are shown displaced from that axis for clarity. From Eq. (25) the absolute effective coordination numbers $N_S(\theta)$ for $\Delta_I(k)=0$ are $\alpha(90°)n_d(90°)=(1.4)(0.5)=0.7$ and $\alpha(0°)n_d(0°)=(0.8)(2.0)=1.6$. The relative SEXAFS amplitude $N_S(0°)/N_S(90°)=2.3$.

It is with the simplifying assumption of $\Delta_I(k)=0$ in Fig. 1(a) that the data of I on Si(111) had been analyzed.[14] The appropriateness of that approach can be assessed by considering the effects of a finite $\Delta_I(k)$. An empirical procedure for determining $\Delta_I(k)$ is given in Sec. III B 2, but an alternate method is to use the values of $\phi_I^{l=0}(k)$ and $\phi_I^{l=2}(k)$ as calculated by Teo and Lee.[25] This is the approach adopted by SJ [these authors used $\phi_{Ag}^{l=0}(k)$ and $\phi_{Ag}^{l=2}(k)$, and $\Delta_{Ag}(k)$ is almost identical to $\Delta_I(k)$]. In Fig. 1(b) the ratios $n_{sd}(0°)/n_d(0°)$ and $n_{sd}(90°)/n_d(90°)$ are shown for the value of Δ_I calculated at $k=7$ Å^{-1}. Other values of Δ_I as a function of k are indicated. Casual inspection of Fig. 1(b) would seem to indicate that the effects of $\Delta_I(k)$ are substantial. This is also the conclusion reached by SJ. The projection of $\alpha(k,0°)$ on the Im axis shows that the total SEXAFS phase is increased, which in the next section will be seen to yield a bond length $R(0°)$ that is *lengthened* relative to the value derived assuming $\Delta_I(k)=0$. For $\theta=90°$ the total phase is decreased by about twice the amount for $\theta=0°$, leading to a *shortening* of the bond length. The absolute value of $\alpha(k,0°)$ is larger than it would have been had $\Delta_I(k)=0$. The result is an *increased* total SEXAFS amplitude $N_S(0°)$ from 1.6 to $(1.08)(2.0)=2.16$. The amplitude $N_S(90°)$ is *decreased* from 0.7 to $(0.95)(0.5)=0.47$. The relative amplitude $N_S(0°)/N_S(90°)$ is, of course, modified even further. Finally, because Δ_I is a function of k, both the SEXAFS distances and relative amplitudes are also k dependent. The central problem concerning this paper can thus be succinctly stated: Bond lengths and effective coordinating numbers determined from $L_{2,3}$-edge SEXAFS data appear to be very different depending upon whether $\Delta_a(k)$ is taken to be zero or finite.

III. DISCUSSION

In view of the problem posed above, four questions must be addressed.

(1) Assuming the calculated $\Delta_a(k)$ values are reliable, to what degree are the derived $L_{2,3}$-edge SEXAFS bond lengths and amplitudes affected for chemisorption systems with the worse-case atop configuration?

(2) To what degree are the calculated $\Delta_a(k)$ values reliable and how does their uncertainty affect the $L_{2,3}$-edge SEXAFS distances and amplitudes for systems with the atop geometry?

(3) To what degree are the effects of the cross term and uncertainties in $\Delta_a(k)$ important for other chemisorption geometries and polarization directions?

(4) Assuming the effects of the cross term are nonnegligible in $L_{2,3}$-edge SEXAFS data, what general analysis procedures can be applied to obtain the most reliable bond lengths and adsorption sites?

These questions are now answered in the order raised.

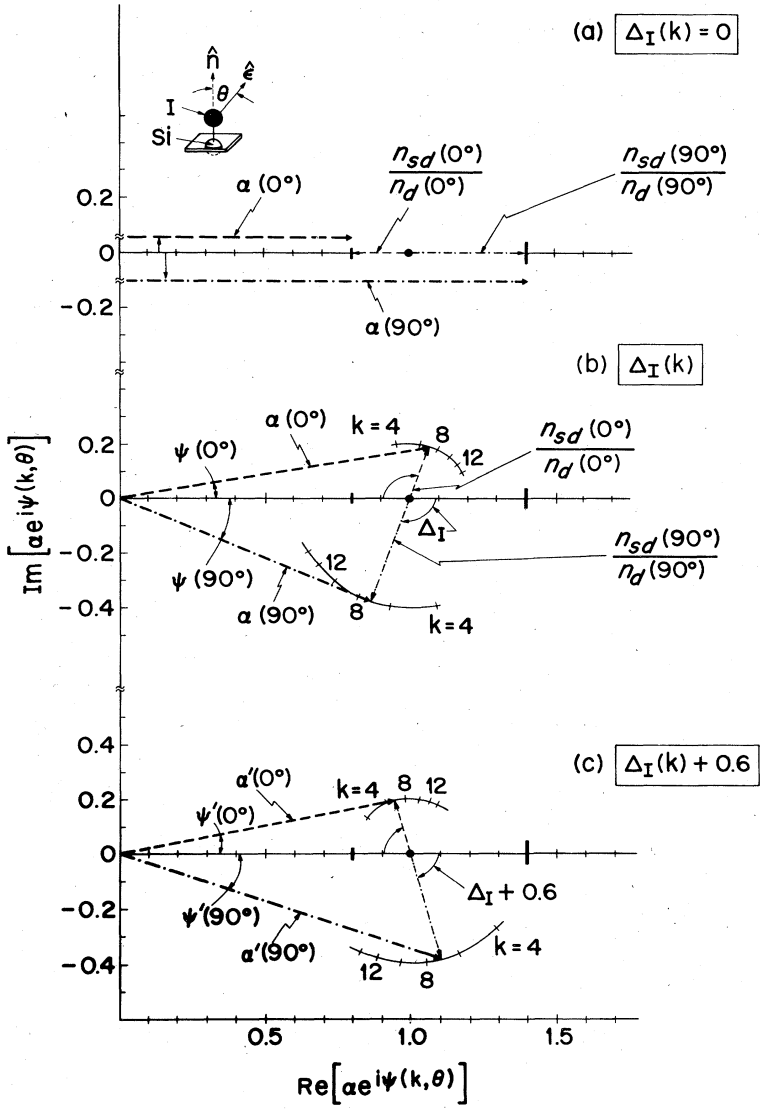

FIG. 1. Phasor diagram illustrating the effect of the total s-d cross term [defined in Eq. (16) and rewritten in Eq. (21)] on the amplitude and phase of the $L_{2,3}$-edge SEXAFS for the case of an adatom in the atop configuration. Shown here is I on Si(111). The SEXAFS amplitude (and thus the coordination number) is affected by the magnitude of $\alpha(k,\theta)$ [Eq. (22)]. It is indicated by bold dashed or dotted-dashed lines for $\theta=0°$ or 90°, respectively. In (a) there is no k dependence of $\alpha(k,\theta)$, in (b) and (c) that quantity is shown at $k=7$ Å^{-1} (its magnitude as a function of k is also indicated). The SEXAFS phase (and thus the bond length) is affected by the angle $\psi(k,\theta)$ [Eq. (23)]. Both $\alpha(k,\theta)$ and $\psi(k,\theta)$ depend on the s-d cross-term phase correction $\Delta(k)$ [Eq. (10)] and on the partial coordination numbers $n_d(\theta)$ and $n_{sd}(\theta)$ [Eqs. (17) and (18)]. The latter reflect the adsorption geometry, the former reflects the difference in phase (i.e., the interference) between the s and d final states waves. If $\Delta(k)=0$, as in case (a), there is no effect on the SEXAFS phase and $\psi(k,\theta)=0$. The SEXAFS amplitude is still affected, however, because $n_{sd}(\theta)$ is nonzero. [For isotropic $L_{2,3}$-edge absorption or when $\theta=54.7°$, $n_{sd}=0$ and $\alpha(k,\theta)=1$.] The ratios of $n_{sd}(\theta)/n_d(\theta)$ for the anisotropic atop configuration are indicated by light dashed ($\theta=0°$) and dotted-dashed ($\theta=90°$) lines lying along the Re axis and are terminated by bold short (0°) and long (90°) vertical fiducial lines. The effect of $n_{sd}\neq 0$ in case (a) is to reduce $\alpha(0°)$ to 0.8 and to increase $\alpha(90°)$ to 1.4. These values of $\alpha(\theta)$ also lie along the Re axis but are shown displaced from it for clarity. In case (b), the calculated values of $\Delta(k)$ for I from Ref. 25 are used (e.g., at $k=7$ Å^{-1}, $\Delta_I\sim -109°$). The finite values of $\psi(k,\theta)$ affect the SEXAFS phase in opposite directions for $\theta=0°$ and 90°. The SEXAFS amplitudes are very strongly affected, with $\alpha(0°)$ increasing and $\alpha(90°)$ decreasing relative to the values in (a). In case (c), if 0.6 rad are uniformly added (see text) to the calculated $\Delta_I(k)$ (e.g., at $k=7$ Å^{-1}, $\Delta_I'\sim -75°$), the values $\psi'(k,\theta)$ are similar to $\psi(k,\theta)$ in (b), but the values $\alpha'(k,\theta)$ approach those in (a). The conditions in (c) more closely approximate the experimental data for I on Si(111) [see Fig. 4(b)].

A. Effect of $\Delta_a(k)$ on bond length and amplitude for atop geometry

1. Simulated data

In Fig. 2(a) are shown simulated SEXAFS data for I on Si(111) in the atop geometry using $R=2.445$ Å and the calculated I and Si phase shifts of Teo and Lee (TL).[30] In order to approximate the actual data more closely, the simulated data have been multiplied by the function $A'(k)$ using TL's backscattering amplitude $f(\pi,k)$ for Si, a value of 0.05 Å for σ, and the relationship $\lambda(k)\approx k$.[31,32] The angles of $\theta=90°$ and 10° and the truncation at $k\sim 8.5$ Å^{-1} were chosen as a compromise between the conditions of the experimental I-Si(111) data[14] discussed in the next section (90°, 35°, 8.2 Å^{-1}), and those of the hypothetical Ag-Si(111) data chosen by SJ (90°, 10°, 9.5 Å^{-1}). Figure 2(a) shows the simulated data with $\Delta_I(k)=0$, Fig. 2(b) shows that with $\Delta_I(k)$ calculated by TL. These conditions are essentially the same as those shown in Figs. 1(a) and 1(b). Simulated data were also constructed for the hypothetical model compound I-Si using the same phase shifts, amplitude function, and bond length, but with $\theta=54.7°$ in order to angularly average the terms in Eq. (16) and obtain $n_d(54.7°)=N=1$ and $n_{sd}(54.7°)=0$. Following standard analysis procedures,[8,9,11,13–18] the derived bond lengths from the two simulated spectra in Fig. 2(a) with $\Delta_I(k)=0$ were reproduced to better than 0.001 Å. For the two simulated spectra in Fig. 2(b) with finite $\Delta_I(k)$, the determined values are different than those for $\Delta_I(k)=0$ and are summarized in Table II. Since SJ used Ag instead of I in the atop position on Si(111) (and $R_{\text{Ag-Si}}=2.5$ Å), the same procedures and distance have also been applied with Ag phase shifts and a Ag-Si model compound. The bond lengths obtained for Ag-Si(111) with finite $\Delta_{Ag}(k)$, see Table II, are not very different than those for I-Si(111) because the TL-calculated phase shifts for I and Ag are quite similar.[25] For comparison, the reported results of SJ for Ag-Si(111) are also shown in Table II. These authors note that for the case of $\theta=90°$, the bond-length discrepancy they obtain of 0.04 Å [compared with the value that would have been obtained with $\Delta_{Ag}(k)=0$] is larger than typical errors of <0.02 Å found from analysis of high-quality experimental data, leading them to conclude that the cross term can significantly affect the derived bond lengths in $L_{2,3}$-edge SEXAFS data. Note, however, that the magnitude of the bond-length discrepancy determined here for $\theta=90°$ in the simulated data is substantially smaller than that found by SJ and is comparable to typical precision limits obtained from experimental data.[9–11,15–18]

TABLE II. Bond-length errors (in Å) due to $\Delta_a(k)\neq 0$ determined from analysis of simulated $L_{2,3}$-edge SEXAFS data with the atop configuration and using phase shifts from Teo and Lee, Ref. 25 (see text for details).

	This work		SJ (Ref. 21)
θ	I-Si(111)	Ag-Si(111)	Ag-Si(111)
10°	0.003	0.004	0.005
90°	−0.015	−0.018	−0.04

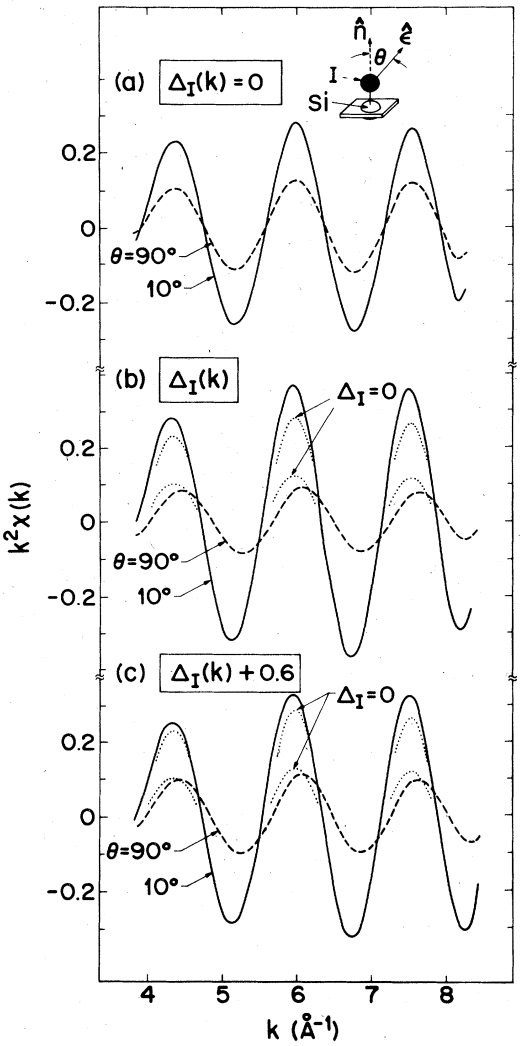

FIG. 2. Simulated L_3-edge SEXAFS data using Eq. (24) for I on Si(111) in the atop configuration. The conditions shown are essentially the same as those in Fig. 1 ($\cos^2 10°\approx\cos^2 0°$). Analysis of the data in (b) gives a difference between the I—Si bond length at $\theta=10°$ and that of 90° of only ~ 0.02 Å, but gives a difference in SEXAFS amplitude ratios of ~ 2 relative to that determined in (a). Analysis of the data in (c) gives a somewhat smaller I—Si bond-length difference but a very much smaller difference in SEXAFS amplitude ratio.

The origin of the larger discrepancy for $R_{\text{Ag-Si}}(90°)$ in the simulated data is traceable to the method used by SJ for determining bond lengths. The variety of methods that exist for deriving distances from EXAFS data have been discussed elsewhere[8,33,34] and are only briefly outlined here. All methods use a model system of known structure from which the EXAFS $\chi(k)$, and ultimately the total phase $\Phi_M(k)=2kR_M+\phi^M_{ab}(k)$, are obtained. The $\chi(k')$ of the system with unknown R is analyzed in an identical manner to give $\Phi(k')=2k'R+\phi_{ab}(k')$. The prime notation indicates a different k scale from the model compound, i.e., the threshold energies E_0 corresponding to $k=0$ in the model and unknown systems are different because they depend sensitively on chemical en-

vironment. Now the concept of phase-shift transferability[24] states that at photoelectron energies above ~ 60 eV ($k \sim 4$ Å^{-1}), where scattering is from core rather than valence electrons, the phase shift $\phi_{ab}(k)$ for a given absorbing-backscattering atom pair is the same regardless of chemical environment. Removal of $\phi_{ab}(k')$ with use of $\phi^M_{ab}(k)$ therefore allows R to be accurately determined provided the k scales in the two systems are matched. The most common methods for accomplishing this scale matching involve (a) adjusting the phase difference $\Phi^M(k)-\Phi(k)$ such that a linear least-squares fit to it extrapolates through $k=0$ (Ref. 8), (b) adjusting the phase difference divided by k, i.e., $[\Phi^M(k)-\Phi(k)]/k$, such that it has zero slope,[35] or (c) adjusting the phase difference such that it is linear as determined by amplitude and phase matching in the individually Fourier-transformed data.[8] SJ use method (b), while method (a) is used here. The independent parameters that can be adjusted, k and E_0, are the same for all three methods but the uncertainties and derived values of R are not. These depend on the length of the data, their signal-to-noise ratio, any differences between $\phi^M_{ab}(k)$ and $\phi_{ab}(k)$, and the manner in which the phase differences are weighted by k. It is these latter two factors that are important in this discussion. For the case of $L_{2,3}$-edge absorption from an *isotropic model* compound and from an *anisotropic unknown* system, the phase difference between $\phi^M_{ab}(k)$ and $\phi_{ab}(k)$ is just the cross-term correction $\Delta_a(k)$. Assuming matched k scales and thus $\Delta E_0=0$, this gives

$$\Phi^M(k)-\Phi(k)=2k(R_M-R)+\phi^M_{ab}(k)-\phi_{ab}(k)$$
$$=2k(R_M-R)-\Delta_a(k)\ .$$

This is a formal statement of the condition that phase-shift transferability is no longer obeyed. To compensate for this condition, i.e., to make it appear that transferability is still operational, both analysis methods (a) and (b) adjust E_0 and R, leading to errors in the bond-length determination. However, because method (b) first divides the phase differences by k and then adjusts R and E_0 to obtain a zero slope, the lower-k data are given greater weight than the higher-k data. If method (b) used k-dependent error bars to balance out this effect, it would clearly be equivalent to method (a), but as that method is conventionally used this k-dependent correction procedure is not performed. Therefore, because method (b) places too much weight on the data at low k, it ultimately overestimates the effect of a finite $\Delta_a(k)$ and thus the magnitude of the error on the derived bond length. This conclusion has been verified by using method (a) on simulated data that had been truncated. Furthermore, even if the total bond-length anisotropy of SJ had been determined using k-dependent error bars, i.e., giving 0.02 Å rather than 0.04—0.05 Å, these values for the worse-case example of atop adsorption still represent upper limits because the value of $|\Delta_a(k)|$ calculated by TL averages around $|\pi/2|$ for both I and Ag, the maximum amount by which $\psi(k)$ can be affected.

The second consequence of a finite $\Delta_a(k)$ on $L_{2,3}$-edge SEXAFS data is a modification of the amplitude, and it appears to be much more important than the modification of the bond length. As discussed in Sec. II C, Fig. 1(b) depicts the situation at $k=7$ Å^{-1} when $N_S(0°)=2.16$ and $N_S(90°)=0.47$. The relative amplitude at this value of k is therefore $N_S(0°)/N_S(90°)=4.6$, *twice* the value of $1.6/0.7=2.3$ obtained with $\Delta_a(k)=0$ in Fig. 1(a). SJ correctly note that such a discrepancy is comparable to the differences in the calculated relative amplitudes for $L_{2,3}$ edges which are used to distinguish between chemisorption sites,[11,14,15,36] and is certainly outside typical error limits of $\pm 10\%$ for relative amplitudes obtained from actual high-quality data.[13–16] However, because these authors do not have such data from a system in which the chemisorption geometry is well established, they cannot reconcile this strong discrepancy between the amplitudes of simulated and real data. Instead, they propose a data-analysis procedure which deserves some clarification here (the actual source of the amplitude discrepancy will be treated in Sec. III B).

Using simulated data, SJ compared the relative amplitudes $N_S(90°)/N_S(10°)$ for Ag on Si(111) in a hypothetical atop geometry for the case of $\Delta_{Ag}(k)=0$ and $\Delta_{Ag}(k)\neq 0$.[37] These conditions are essentially identical to those for I on Si(111) shown in Figs. 1(a) and 1(b) for $\theta=90°$ and 0° and

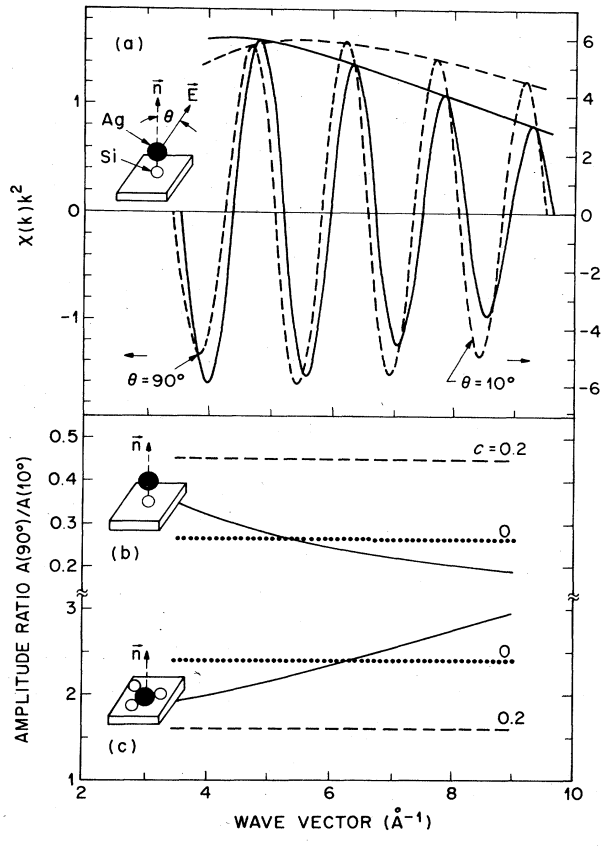

FIG. 3. From Ref. 21. (a) Simulated L_3-edge data for Ag in the atop configuration on Si, similar to the conditions of I on Si in Figs. 1 and 2. Note different amplitude scales for the different spectra. (b) SEXAFS amplitude ratio of the data in (a) (solid line) compared with that ratio assuming $c=0.2$ (dashed line) and $c=0$ (dotted line). The approximation labeled $c=0.2$ corresponds to $\Delta(k)=0$ used in the present work. (c) Same comparison for the case of Ag in a coplanar configuration.

in Figs. 2(a) and 2(b) for $\theta=90°$ and 10°. The comparison of SJ is reproduced in Fig. 3(a). In addition to the large magnitude of the relative amplitude discrepancy discussed above for the cases of a finite and a zero $\Delta_{Ag}(k)$, the k dependence of the relative amplitude for finite $\Delta_{Ag}(k)$ has been made more apparent by normalizing the simulated data for the different values of θ (note different scales). SJ point out that by setting the ratio $c=M_{01}/M_{21}=0$ rather than to 0.2, a relative amplitude is obtained which intersects the one for finite $\Delta_{Ag}(k)$ at $k\sim 6$ Å^{-1}, see Fig. 3(b). This agreement has been used elsewhere[36] to justify the approximation of $c=0$ in the analysis of relative amplitudes of experimental SEXAFS data for Ag on Si(111) (this analysis will be discussed further in Sec. III C). The procedure of using $c=0$ seems counterintuitive, since there is both theoretical[25] and experimental[20] evidence that c is indeed ~ 0.2. The origin of the agreement at $k\sim 6$ Å^{-1}, however, lies in the use of the TL-calculated $\Delta_a(k)$ for Ag or I. From Fig. 1(b) this calculated value is seen to average around $-\pi/2$ for $4\lesssim k\lesssim 8$ Å^{-1}. Substitution of $-\pi/2$ for $\Delta_a(k)$ in Eq. (25) gives $N_S(\theta)=[n_d(\theta)^2+n_{sd}(\theta)^2]^{1/2}\approx n_d(\theta)$, making it appear that $n_{sd}(\theta)=0$. Ironically, using the TL-calculated value of $\Delta_a(k)$ in the analysis of Ag (or I) $L_{2,3}$-edge SEXAFS amplitudes appears to be equivalent to setting the entire value of the cross term equal to *zero*, just as in isotropic $L_{2,3}$-edge absorption.

2. *Experimental data*

The simple procedure above proposed by SJ for analyzing $L_{2,3}$-edge SEXAFS amplitudes is based on two (related) assumptions: (1) the TL-calculated value of $\Delta_a(k)$ is accurate, and (2) the analysis of such data using $\Delta_a(k)=0$, i.e., Eqs. (19) and (20), can lead to significant errors. As mentioned, these authors[21] do not have experimental SEXAFS data from a system in which the chemisorption geometry is clearly established and so they cannot test either of these assumptions. The question of the accuracy of the calculated $\Delta_a(k)$ values will be treated in the next section. Here, experimental data from a system with unambiguous atop geometry are examined to see whether the large effects predicted by SJ using calculated $\Delta_a(k)$ values are actually observed.

Figure 4(a) shows the raw background-subtracted SEXAFS L_3-edge data of Si(111)7×7–I for $\theta=90°$ and 35°.[14] The upper limit of $k\lesssim 8.5$ Å is established by the I L_2 edge. The Fourier transforms of that data are shown in Fig. 5 along with the two window functions used to isolate the first-neighbor I-Si bond length from the second-neighbor I-Si distance and the higher-frequency noise components. The filtered back-transformed data using the first-neighbor window function are shown as solid lines superposed on the raw data in Fig. 4(a). The differences between the raw and filtered data, particularly at low k, are due to the additional SEXAFS from the *second*-neighbor Si atoms. The first-neighbor filtered data are directly compared in Fig. 4(b). Also shown in Figs. 4 and 5 are analogous data for the model compound $SiI(CH_3)_3$.[14]

Qualitative comparison between the data for the model and surface systems shows that the bond lengths are similar. Quantitatively, a difference in the phases for the $\theta=35°$ and 90° data is observed in Fig. 4(b) which resembles that shown in Fig. 2(b). This phase difference corresponds to a total relative bond-length difference of 0.021 Å. The absolute I-Si(111) bond lengths are determined using the I-Si distance of 2.46±0.02 Å in $SiI(CH_3)_3$,[38] giving $2.43_4\pm 0.02_5$ Å for $\theta=90°$ and $2.45_5\pm 0.02_5$ Å for $\theta=35°$ (this explains the choice of $R=2.445$ Å in the simulated data). In Sec. III D a general method for removing even this small bond-length anisotropy is described, but for now it is sufficient to note that the quoted I-Si(111) bond length[14] is the same as the

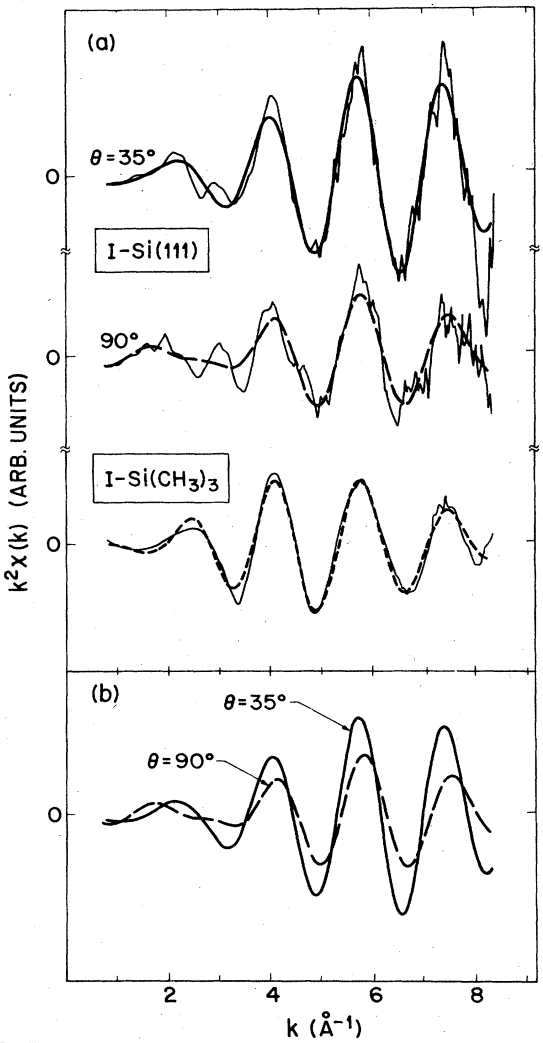

FIG. 4. Experimental I L_3-edge data from Ref. 14. The raw background-subtracted data correspond to a saturation coverage ($\lesssim 1$ ML) of I on Si(111)7×7 and to a bulk concentration of I in the condensed vapor $SiI(CH_3)_3$. The smooth bold curves superposed on the raw data represent back-transformed filtered data from the first-neighbor peaks in the Fourier transforms (see Fig. 5). The discrepancies between the raw and filtered I/Si(111) data arise from contributions from the second-neighbor Si atoms. The direct comparison of the filtered data in (b) shows a small anisotropy in the phases similar to that seen in Fig. 2(b).

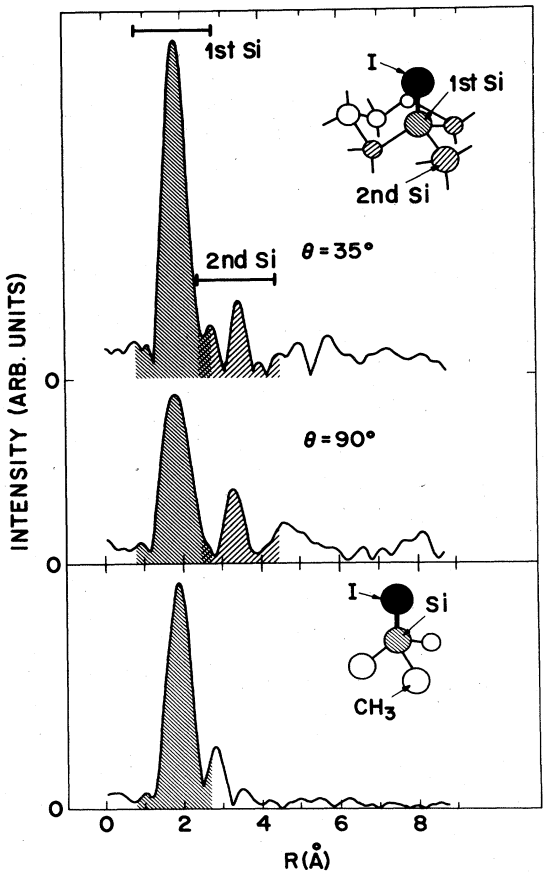

FIG. 5. Fourier transform of data in Fig. 4. A smooth window function from $R=0.8$ Å to 2.8 Å is used to isolate the first-neighbor Si contribution from the other Fourier components. The second-neighbor Si contribution in the I-Si(111) system is apparent in both the $\theta=35°$ and 90° transforms [the peak at ~2.9 Å in the $SiI(CH_3)_3$ data corresponds to I-C scattering].

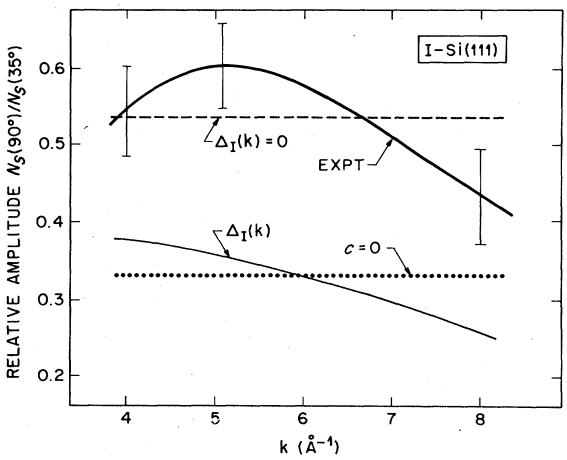

FIG. 6. Comparison between the experimental SEXAFS amplitude ratio from the I-Si(111) data (Ref. 14 and Fig. 4) with the predictions of Eq. (25) using (i) the calculated value of $\Delta_I(k)$ (Ref. 25), (ii) $\Delta_I(k)=0$, and (iii) $c=0$. The functions for I-Si(111) are plotted analogous to those for the hypothetical Ag-Si(111) data in Fig. 3(b) [the approximation here of $\Delta_I(k)=0$ corresponds to $c=0.2$ used in that figure and in Ref. 21]. Conditions (i) and (iii) agree with one another here as well as in Fig. 3(b) (see text for explanation), but both fall outside the error bars of the experimental curve. Only the calculated SEXAFS amplitude ratio assuming $\Delta_I(k)=0$ overlaps with experiment.

average of the two different values, i.e., 2.44±0.03 Å. The effect of the cross term on the bond length is thus seen to produce a total anisotropy of 0.02 Å, or an imprecision ±0.01 Å. Although this uncertainty is small compared to the total quoted uncertainty of ±0.03 Å (due mainly to the imprecise distance[38] of the model compound), it is larger than usual *relative* uncertainties of ±0.005 Å measured in other systems.[11,13,15,18] Thus the observed[14] bond-length anisotropy (0.02_1 Å) is comparable to that determined[39] in the preceding section from simulated data (0.018 Å) and is, as discussed above, about half as large as that determined by SJ (0.045 Å) using essentially the same simulated data with a different analysis procedure.

The similarity between the experimentally observed effect of the cross term on the bond length and that determined here from simulated data might suggest a corresponding similarity in the amplitude, but this is certainly *not* the case. The experimental relative amplitude $N_S(90°)/N_S(35°)$ for Si(111)7×7—I is compared in Fig. 6 with that predicted from Eq. (16) using $\Delta_I(k)=0$ and using the value of $\Delta_I(k)$ calculated by TL. The functions have been plotted analogous to those in Fig. 3(b) to facilitate comparison.[37] Error bars are indicated in Fig. 6 to account for the dependence of the relative amplitude on statistical noise and systematic uncertainties, e.g., the functional forms of the subtracted background and window function. Even allowing for these errors, the overall magnitude of the experimental curve is seen to be inconsistent with that from Eq. (16) using the calculated value of $\Delta_I(k)$ or using the approximation of $c=0$. There is, however, good agreement in the average value of the data using the approximation of $\Delta_I(k)=0$. This conclusion is exactly opposite to that suggested by SJ on the basis of their analysis of simulated data shown in Fig. 3. The possibility that the Si(111)7×7—I system is not representative of an atop configuration is completely ruled out by the clear observation of a second-neighbor I-Si(111) distance[14] corresponding to only this geometry. Furthermore, the absolute SEXAFS amplitudes $N_S(35°)$ and $N_S(90°)$ determined from comparison with the value of $N=1$ in $SiI(CH_3)_3$ independently establish the adsorption site to be atop.[14] Similar results have also been obtained in the system Ge(111)1×1—I.[14]

The fact that there is an observed k dependence of the relative amplitude for both systems, as well as a small polarization dependence of the bond length, suggests that $\Delta_I(k)$ is finite rather than zero. This question is explored more fully in the next section. The point to be made here, however, is that the predictions of the cross term on the relative amplitude are *not correct* using the value of $\Delta_I(k)$ calculated by TL. Furthermore, the experimental relative amplitude is closely approximated by taking $\Delta_I(k)=0$ and $c=0.2$, *not* $c=0$. The apparent paradox of these findings is that the small but finite calculated effect of the

cross term on the bond length is observed, but the much larger calculated effect of the cross term on the amplitudes is most definitely not.

B. Accuracy of calculated $\Delta_a(k)$

An important point emphasized in this work, and apparently not recognized by SJ, is that the $L_{2,3}$-edge SEXAFS amplitude is very strongly dependent on the value of $\Delta_a(k)$, see Figs. 1(a) and 1(b). The purpose of this section is to demonstrate that the source of the discrepancy found in the previous section between the amplitudes of the simulated and the experimental data lies in the accuracy of the calculated $\Delta_a(k)$.

There is no direct empirical method for determining the individual absorbing atom phase shifts $\phi_a^{l=0}(k)$ and $\phi_a^{l=2}$, but there are two methods for determining the uncertainties of $\Delta_a(k)$ which are suggested from the following considerations. Calculated total phase shifts $\phi_{ab}^{l=1}(k)$ and $\phi_{ab}^{l=2}(k)$ are routinely used in the analysis of EXAFS data[2–8] when model compounds are not available, and the accuracies of such calculated phase shifts have been recently tested[34] by comparing determined bond lengths in a variety of model systems with the known values. The bond-length errors so obtained in this latter study, typically 0.02—0.05 Å, were stated[34] to correspond to errors of $\sim$5—15% in the total phase shift, but these percentages can be misleading since the relative errors strongly depend on the system in question. For example, in bulk CuBr the total phase-shift contribution to the Br K-edge EXAFS in the range $4<k<9$ Å^{-1} is $\sim$0.3 Å, so an error of 0.03 Å in the distance does correspond to a 10% error in $\phi_{\mathrm{BrCu}}^{l=1}(k)$. For the case of bulk Pd, on the other hand, the total phase-shift contribution to the Pd K-edge EXAFS in the same k range is only $\sim$0.05 Å, so the same 0.03 Å error represents a substantially larger relative error. The reason for the different total phase-shift contributions in these two examples is that the backscattering phase shifts $\phi_b(k)$ have k-dependent slopes of opposite sign. This suggests that to estimate the errors in $\Delta_a(k)$, which depends only on the phase shifts of the absorbing atom, the effect of $\phi_b(k)$ should be removed. One of the two methods by which this can be accomplished is to compare calculated and experimental total phase shift *differences* from different absorption edges in the *same* system.

An example of this procedure is given for bulk CuI. Filtered experimental EXAFS data from the I L_1 and L_3 edges of CuI are shown by bold lines in the upper half of Fig. 7. Superposed on these data with light lines are simulated CuI data using the calculated phase shifts of TL and an amplitude function as described for the I-Si(111) system. By subtracting $2kR_{\mathrm{ICu}}$ from the total phase of the real data, the total phase shifts $\phi_{\mathrm{ICu}}^{l=1}(k)$ and $\phi_{\mathrm{ICu}}^{l=2}(k)$ are obtained. The backscattering phase shift $\phi_{\mathrm{Cu}}(k)$ cancels in their difference to give $\phi_{\mathrm{I}}^{l=1}(k)-\phi_{\mathrm{I}}^{l=2}(k)$. Analogous to Eq. (10), this difference is defined as

$$\Delta_a^*(k)=\phi_a^{l=1}(k)-\phi_a^{l=2}(k)\ . \tag{26}$$

The experimental total phase shifts and the value $\Delta_I^*(k)$ are shown in the lower half of Fig. 7 and are compared

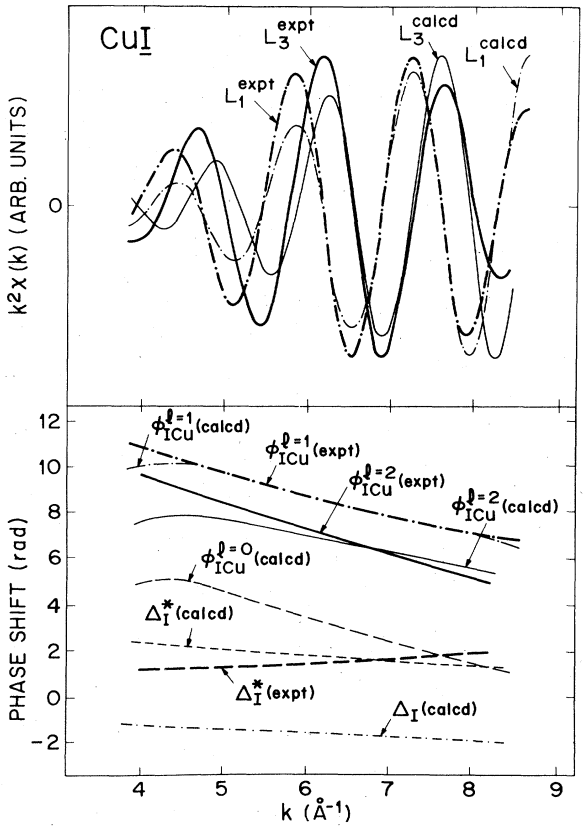

FIG. 7. Determination of experimental $\Delta_I^*(k)$ value [Eq. (26)] and comparison with theory. In the upper half, I L_1- and L_3-edge filtered EXAFS data from bulk CuI (bold dotted-dashed and solid lines) are compared with corresponding simulated data (light dotted-dashed and solid lines), showing qualitatively good agreement. The calculated total (central and backscattered atom) phase shifts from Ref. 25 used in generating the simulated data are shown in the lower half. These, in turn, are compared with the experimental total phase shifts, showing very good agreement for $\phi_{\mathrm{ICu}}^{l=1}(k)$ and poorer agreement for $\phi_{\mathrm{ICu}}^{l=2}(k)$. The calculated central-atom phase shift differences $\Delta_I^*(k)$ are also compared with the experimental value, obtained by taking the difference between the total phases for the L_1-edge and L_3-edge data [i.e., the backscattering phase shift $\phi_{\mathrm{Cu}}(k)$ cancels]. The lack of quantitative agreement is apparent. The inability to obtain data containing only $\phi_{\mathrm{I}}^{l=0}(k)$ precludes empirical determination of $\Delta_{\mathrm{I}}(k)$ [Eq. (10)] from bulk measurements using these procedures; only the calculated quantities are shown.

with those quantities as calculated by TL. Also shown are the calculated values of $\phi_{\mathrm{ICu}}^{l=0}(k)$ and $\Delta_{\mathrm{I}}(k)$. Note that the actual ordering of the phase shifts shown in Fig. 7 is arbitrary, since all are modular 2π. Comparison between the real and simulated EXAFS data shows qualitatively good agreement. Quantitatively, however, the experimental and theoretical values for $\phi_{\mathrm{I}}^{l=2}(k)$ and for $\Delta_I^*(k)$ are quite different. Looking at $\Delta_{\mathrm{I}}^*(k)$, the functions are about equal at $k\sim7$ Å^{-1}, at $k=6$ or 8 Å^{-1} they differ by $\sim$0.4 rad, and at $k=5$ or 9 Å^{-1} they differ by $\sim$0.9 rad. Three questions emerge: (i) Are the differences between the cal-

culated and experimental $\Delta_I^*(k)$ values shown in Fig. 7 real? (ii) Are these differences unique to I? (iii) Are these differences significant to the effect of the s-d cross term?

In answering question (i), there are two ways to test the reliability of the experimental $\Delta_I^*(k)$ value. Since EXAFS from two different edges are being compared, even if from the same system, the choice of E_0 for each edge will affect the value of Δ_I^*; this is a test of precision. Variations of E_0 as large as ± 10 eV were chosen for the different edges, with the largest change on the experimental $\Delta_I^*(k)$ being the essential removal of its k dependence and an overall displacement to less negative values. The net effect actually worsens the agreement between the experimental and calculated values and therefore changing E_0 does not remove the discrepancy. The absolute accuracy of the individual experimental phase shifts $\phi_I^{l=1}(k)$ and $\phi_I^{l=2}(k)$ can only be tested by comparing calculated bond lengths with known values, and this means adding to each central-atom phase shift the additionally uncertain calculated value of $\phi_b(k)$. By deriving bond lengths from different edges in the same systems, i.e., with the same $\phi_b(k)$, this problem is at least partially minimized. From the L_1-edge EXAFS data and the appropriately calculated total phase shift, the I-Cu distance was determined to be within 0.01 Å of the experimental value. However, for the L_3-edge data the error was 0.09 Å (the calculated values are all too small). The good agreement obtained for the L_1 edge and poor agreement for the L_3 edge does *not* establish that the source of error lies *solely* in $\phi_I^{l=2}(k)$, since either a cancellation or an accumulation of errors in $\phi_a(k)$ and $\phi_b(k)$ cannot be ruled out. As an example of testing the effect of $\phi_b(k)$, the I L_3-edge EXAFS data from I-Si$(CH_3)_3$ was analyzed, giving an error of 0.04 Å between the known and derived I-Si bond lengths. This error is smaller than that found for I-Cu, attesting to the fact that the effect of $\phi_b(k)$ is non-negligible. Despite the fact that there is no method for determining the distribution of errors between two different kinds of phase shifts (backscattering and central atom), the above analysis from different edges in the same system shows that regardless of $\phi_b(k)$, there must be some inaccuracy in the calculated $\phi_I^{l=2}(k)$ value which appears to be larger than that of $\phi_I^{l=1}(k)$ and which cannot be removed by changing E_0.

In answering question (ii), the inaccuracy of $\Delta^*(k)$ for elements other than I has been tested by analyzing L_1- and L_3-edge EXAFS data from bulk Ag. Again, a discrepancy between the calculated and experimental values of $\Delta_{Ag}^*(k)$ was found (it is larger than that for I). Furthermore, a test of the accuracy of the central-atom phase shifts for Ag gave results opposite to that for I in CuI, i.e., the Ag-Ag bond length was within 0.01 Å of the known value using the L_3-edge data whereas the Ag-Ag bond length error using the L_1 edge was 0.11 Å. This result has also been found in an independent analysis of Ag K-edge data,[33] where the inaccuracy of the calculated total phase shift using $\phi_{Ag}^{l=1}(k)$ led to an error of 0.10 Å.[40] The inaccuracy of $\phi_{Ag}^{l=1}(k)$ thus appears to be greater than that of $\phi_{Ag}^{l=2}(k)$ [there is no experimental test of $\phi_{Ag}^{l=0}(k)$]. The conclusion to be drawn from the sum of these findings is that for I and Ag there are non-negligible inaccuracies in the calculated central-atom phase shifts $\phi_a^{l=1}(k)$ and $\phi_a^{l=2}(k)$.[41] These inaccuracies can, in some cases, lead to bond-length errors as large as 0.1 Å.

In addressing question (iii), it is important not to confuse the effects of inaccurately calculated central-atom phase shifts on bond lengths, which depend on $\phi_b(k)$, with the effects of such inaccuracies on $\Delta_a(k)$, which do not. This was the reason for introducing the parameter $\Delta_a^*(k)$. Having established with isotropic model compounds that the calculated $\Delta_I^*(k)$ is in error, the question still remains as to how significant the effect of the cross term in anisotropic systems would be if comparable errors existed in $\Delta_a(k)$. To evaluate this most simply, assume that the errors in $\Delta_I^*(k)$ are the same for $\Delta_I(k)$, and that from Fig. 7 these can be approximated by an average "correction" value of ~ 0.6 rad. Uniformly adding this amount to the TL-calculated quantity $\Delta_I(k=7)$ modifies the values of $\alpha(k,\theta)$ and $\psi(k,\theta)$ to $\alpha'(k,\theta)$ and $\psi'(k,\theta)$, and these are shown for $\theta=0°$ and 90° at $k=7$ Å^{-1} in Fig. 1(c). The effect of using this "corrected" cross term is also shown in the simulated I-Si(111) SEXAFS data for $\theta=10°$ and 90° in Fig. 2(c). It is apparent from both these figures that $\psi(k,\theta)$—and thus the bond length—is little affected by this small change in $\Delta_I(k)$. However, the affect on $\alpha(k,\theta)$—and thus the coordination number—is dramatic. Specifically, the effective coordination numbers and relative amplitude $N_S(0°)/N_S(90°)$ at $k=7$ Å^{-1} change from $2.16/0.47=4.6$ in Fig. 1(b) to $1.94/0.58=3.3$ in Fig. 1(c). Such a change is more than half that seen between using the TL-calculated value of $\Delta_I(k)$ and using $\Delta_I(k)=0$ as in Fig. 1(a), i.e., $1.6/0.7=2.3$. Beyond the details of the correction itself (see below), it is clear that the amplitudes of the $L_{2,3}$-edge SEXAFS data are very strongly dependent on the absolute value of $\Delta_a(k)$. This implies that for a reliable assessment of its accuracy, $\Delta_a(k)$ needs to be determined directly. This is the second method alluded to in the beginning of this section.

The empirical procedure for measuring $\Delta_a(k)$ is suggested from the above determination of $\Delta_a^*(k)$, namely, taking difference spectra within a given system. Here the SEXAFS (or EXAFS) is measured with two different polarization angles, θ_1 and θ_2, from the same system whose structure is known and is anisotropic. It is then easy to see from Eq. (16) that with two measurements,

$$\begin{aligned}[A'(k)]^{-1}\chi(k,\theta_1)&=n_d(\theta_1)\sin[2kR+\phi_{2b}(k)]\\&\quad+n_{sd}(\theta_1)\sin[2kR+\phi_{2b}(k)\\&\quad+\Delta_a(k)]\,,\\[A'(k)]^{-1}\chi(k,\theta_2)&=n_d(\theta_2)\sin[2kR+\phi_{2b}(k)]\\&\quad+n_{sd}(\theta_2)\sin[2kR+\phi_{2b}(k)\\&\quad+\Delta_a(k)]\,,\end{aligned}\tag{27}$$

the following difference spectra can be obtained:

$$\begin{aligned}[A'(k)]^{-1}\{\chi(k,\theta_1)-[n_{sd}(\theta_1)/n_{sd}(\theta_2)]\chi(k,\theta_2)\}\\=N^*\sin[2kR+\phi_{2b}(k)]\,,\end{aligned}\tag{28}$$

$$N^*=n_d(\theta_1)-n_d(\theta_2)n_{sd}(\theta_1)/n_{sd}(\theta_2)\,,$$

and

$$[A'(k)]^{-1}\{\chi(k,\theta_1)-[n_d(\theta_1)/n_d(\theta_2)]\chi(k,\theta_2)\} = N^{**}\sin[2kR+\phi_{2b}(k)+\Delta_a(k)] \quad (29)$$

$$N^{**}=n_{sd}(\theta_1)-n_{sd}(\theta_2)n_d(\theta_1)/n_d(\theta_2)\ .$$

Now the difference in total phases (i.e., the arguments in square brackets) between the linearly combined spectra, Eqs. (28) and (29), is simply $\Delta_a(k)$. Note that an advantage of this second procedure over the above empirical determination of $\phi_{ab}^{I=2}(k)$ or $\Delta_a^*(k)$ (a=I, b=Cu) is that the same absorption edge, and thus the same k scales and E_0 values,[42] apply to both measurements.

An example of this procedure is applied to the atop configuration of I on Si(111). Its structure is anisotropic and well established from second-neighbor distances and from relative and absolute amplitudes.[14] A direct comparison of the TL-calculated and empirically derived values of $\Delta_I(k)$ is shown in Fig. 8. As opposed to the comparison in Fig. 7 for $\Delta_I^*(k)$, there is reasonable agreement in the k dependence of these functions,[43] but similar to the case of $\Delta_I^*(k)$ there is a clear and approximately uniform difference in their average values. Error bars are difficult to estimate in difference spectra (particularly near the truncation points), but the uniform discrepancy shown in Fig. 8 has been found to be relatively insensitive to systematic treatment of the data. To quantify the effect of the error in the cross term, the calculated relative amplitude $N_S(35°)/N_S(90°)$ is plotted in Fig. 9 as a function of a mean "correction" value which is added to the calculated quantity $\Delta_I(k=7)$ [the choice of $k=7$ facilitates comparison with Figs. 1(b) and 1(c)]. Note that the calculated relative amplitudes plotted here are the reciprocal of those in Fig. 6. With zero correction added to $\Delta_I(k=7)$ the predicted relative amplitude is 3.3. Adding 0.6 rad decreases this to ~2.6, and adding 1 rad decreases it further to ~2.2. The average observed[14] value of

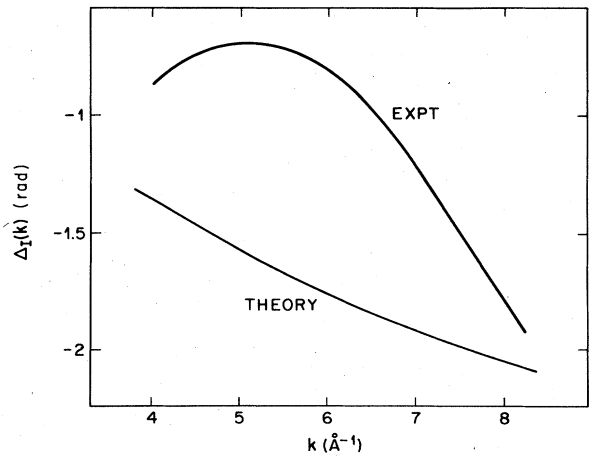

FIG. 8. Comparison between experimental and calculated (Ref. 25) value of $\Delta_I(k)$ [Eq. (10)]. The experimental function is determined from the difference of linearly combined SEXAFS data taken at different polarizations [Eqs. (27)—(29)]. The lack of quantitative agreement for the two functions is evident and is relatively insensitive to systematic errors.

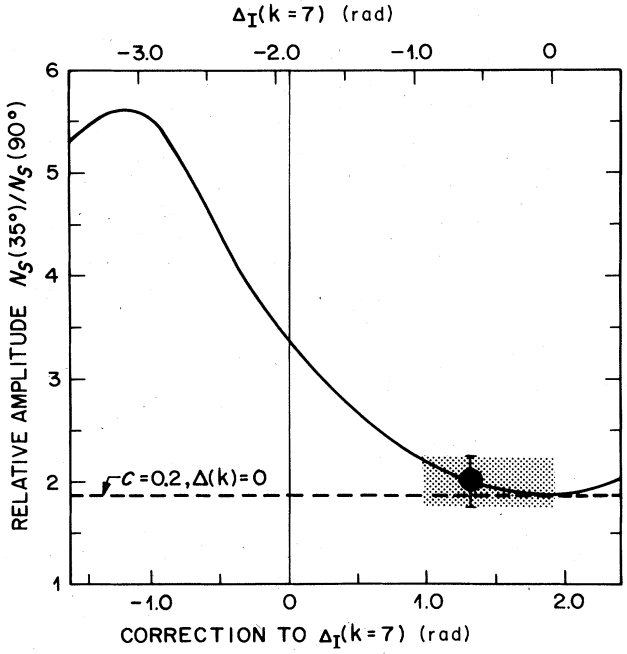

FIG. 9. Dependence of the predicted SEXAFS amplitude ratio on the absolute value of $\Delta_I(k)$, evaluated at $k=7$ Å^{-1}. The conditions for which the amplitude ratio is calculated [Eq. (25)] match the I-Si(111) system (Ref. 14, Fig. 4), i.e., I in the atop geometry. The calculated Δ_I ($k=7$) value from Ref. 25 (see Fig. 8) predicts an amplitude ratio of 3.3 [the reciprocal of this ratio is plotted in Fig. 6 for the curve labeled $\Delta_I(k)$]. A constant positive correction to $\Delta_I(k=7)$ is necessary to bring the predicted amplitude ratios into closer agreement with the experimental value, indicated by the hatched region. The consistency between the approximation of $\Delta_I(k)=0$ (dashed line) and the hatched experimental region corresponds to the curve crossing in Fig. 6.

2.0±0.2 delineates the hatched region in Fig. 9, which defines the experimentally compatible values of Δ_I ($k=7$) and thus the magnitude and sign of the needed correction. As noted in Sec. III A 2, the approximation of $\Delta_I(k)=0$ (dashed line in Fig. 9) gives excellent agreement with the *average* experimental relative amplitude. However, the polarization dependence of the SEXAFS phase for Si(111)7×7—I (Fig. 4) and the k dependence of the relative amplitude (Fig. 6) are both consistent with the empirical determination in Fig. 8 of $\Delta_I(k)$ *not* being zero. Therefore, the strong discrepancy observed between the I-Si(111) data and the predictions using the TL-calculated $\Delta_I(k)$, along with the evidence that $\Delta_I(k)$ is nonzero, is understood by recognizing that the actual value of $\Delta_I(4<k<8$ Å$^{-1})$ is approximately half that calculated by TL, lying in the range of about -1 rad.

These findings are summarized in Fig. 10, where the experimental relative amplitude $N_S(35°)/N_S(90°)$ from Si(111)7×7—I is compared with various calculated amplitudes. As in Fig. 6, using $c=0$ in the cross term, which is equivalent to setting the entire cross term equal to zero, is the least satisfactory approximation. The TL-calculated value of $\Delta_I(k)$ gives good agreement in the k dependence of the amplitude but unacceptably poor agreement in the absolute magnitude. The approximation of

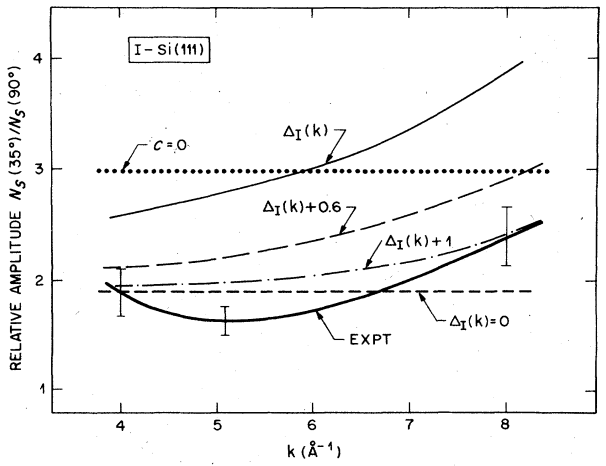

FIG. 10. Same as Fig. 6 but with the reciprocal of the SEXAFS amplitude ratio plotted and with the corrected values of $\Delta_I(k)$ shown. The experimental function is consistent with a corrected $\Delta_I(k)$ and with the approximation of $\Delta_I(k)=0$.

$\Delta_I(k)=0$, which is next simplest, gives very good agreement in the average magnitude but poorer agreement in the slope. A reasonable compromise is obtained using a value of $\Delta_I(k)$ with about a 1 rad correction. The main conclusion from these results, then, and the essential point of this section, is that the inconsistency between the amplitudes of the real data in Fig. 4 and those predicted using the TL-calculated value of $\Delta_I(k)$ is almost entirely due to the inaccuracies of the calculated central-atom phase shifts.

C. Effects of $\Delta_a(k)$ for other geometries

The preceding section has established that for atoms in the atop geometry the effect of the *s-d* cross term on $L_{2,3}$-edge SEXAFS amplitudes depends very strongly on the value of $\Delta_a(k)$. Using calculated central-atom phase shifts to analyze SEXAFS data for atoms in this geometry, therefore, places unreasonably stringent demands on their accuracy. More reliable empirical analysis procedures are given in the following section. Here the question is explored as to how sensitive the effect of the cross term is for atoms in other geometries. If the effects of the cross term are important for these other geometries it could be possible to determine empirically the value of $\Delta_a(k)$ as was done for the case of I-Si(111). If, on the other hand, the effects of the cross term in these other geometries are unimportant, then the exact nature of $\Delta_a(k)$ should be of lesser consequence. In the discussion below, the absorbing atoms I, Te, and Ag are considered because SEXAFS data from them are available for comparison with theory. Also, for simplicity all calculated phase shifts are assumed to be completely accurate.

Following SJ, there is a concise way to illustrate the effect of the cross term for any adsorption geometry with greater than twofold symmetry around the surface normal $\hat{n}$. The angle between $\hat{n}$ and the unit vector along the adsorbate-substrate bond $\hat{r}$ is defined as the bond angle β. This then gives

$$\sum_{i=1}^{N} |\hat{\epsilon}\cdot\hat{r}_i|^2 = N(\cos^2\theta\cos^2\beta + \tfrac{1}{2}\sin^2\theta\sin^2\beta) . \quad (30)$$

Substituting Eq. (30) into Eqs. (17) and (18) allows the relative sizes of the effective partial coordinate numbers $n_d(\theta)$ and $n_{sd}(\theta)$ to be plotted as a function of β and θ. SJ have done this and, using the notation of the present work, their plot is redrawn in Fig. 11 [SJ used the quantities $C_2(\theta)$ $(=n_d(\theta)/N)$ and $C_{02}(\theta)$ $(=n_{sd}(\theta)/N)$]. These authors have chosen the criterion that when the ratio $n_{sd}(\theta)/n_d(\theta)$ is greater than 10% the effect of the cross term cannot be ignored. The adsorption geometries in which the β or θ values produce this condition are indicated by the shaded regions in Fig. 11. Only for those geometries falling within the unshaded region do SJ regard the approximation $\Delta_a(k)=0$ to be valid.

It is possible to test the above criterion for deciding which adsorption geometries are sensitive to the effects of the cross term. In Fig. 11, open and filled symbols have been included to represent the geometries determined from previous SEXAFS measurements. The circles correspond to the onefold atop position of I on Si(111),[14] the triangles and squares represent the threefold and fourfold hollow geometries of I on Cu(111) and Cu(100),[11] and the hexagons represent the sixfold quasicoplanar hollow site of Te on Cu(111) (Ref. 15) [as with $\Delta_{Ag}(k)$, the value of $\Delta_{Te}(k)$ is virtually indistinguishable from $\Delta_I(k)$]. According to SJ, only the I-Cu(100) geometry is sufficiently iso-

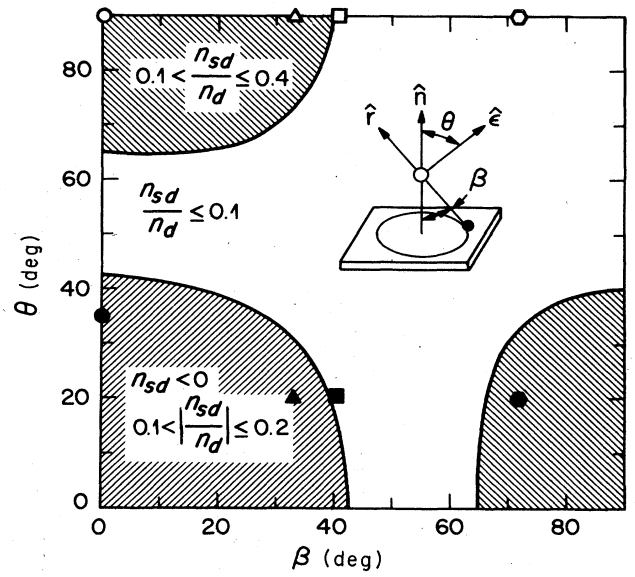

FIG. 11. Effect of the *s-d* cross term as a function of adsorption geometry and polarization, taken from Ref. 21 but modified with the notation from the present work. The cross term is expected (Ref. 21) to be important for those adsorption geometries with corresponding values of $n_{sd}/n_{sd} > 10\%$, indicated by the shaded regions. Added to this figure are geometric shapes representing experimental adsorption geometries and polarization measurements: *circles*: onefold atop, I-Si(111), Ref. 14; *triangles*: threefold hollow, I-Cu(111), Ref. 11; *squares*: fourfold hollow, I-Cu(100), Ref. 11; *hexagons*: quasisixfold substitutional, Te-Cu(111), Ref. 15.

tropic to assume that $\Delta_I(k)=0$ because only it falls in the unshaded region. The relative amplitudes $N_S(20°)/N_S(90°)$ determined from data simulating the experimental threefold, fourfold, and sixfold geometries have been plotted in Fig. 12 for the three conditions $c=0$, $\Delta_I(k)=0$, and $\Delta_I(k)\neq 0$ (see Fig. 10 for the analogous plot of the onefold geometry). The experimentally observed k-averaged relative amplitudes and their error bars have been indicated on these plots at some arbitrary intermediate value of k. For the cases of I on Cu(111) and I on Cu(100), all three conditions fall within the corresponding error limits. The size of the errors from these earlier measurements[11] could now be reduced with better normalization procedures and better signal-to-noise quality under dedicated synchrotron radiation conditions. The smaller error bars in the more recent SEXAFS measurements[15] from Te on Cu(111) taken under these better conditions reflect this fact. Nevertheless, unavoidable systematic uncertainties in the measurement of relative amplitudes from even high-quality data preclude such errors from becoming much smaller than $\sim 10\%$. Within these limits, then, it may be possible to distinguish between the conditions of $\Delta_I(k)\neq 0$, $\Delta_I(k)=0$, and $c=0$ for the threefold hollow geometry, but for the I-Cu(111) data shown in Fig. 12 this is not the case. A much more polarization-dependent geometry is required for assessing the detailed nature of the cross term, and it is for this reason that the atop geometry was used in the preceding section. SJ considered the atop geometry but they did not have experimental data with which to compare their simulations. Instead, they and co-workers[36] used the quasicoplanar geometry of Ag on Si(111) for which they have made measurements. Their assigned configuration for a particular coverage of Ag is essentially the same as that found[15] for Te on Cu(111) and thus falls within the same shaded region in Fig. 11. In Fig. 12 there is agreement between the experimental data of Te on Cu(111) and the curve labeled $\Delta_I(k)=0$, not with the curves labeled $\Delta_I(k)$ or $c=0$. This conclusion is opposite to that reached by Stöhr *et al.*[36] To understand the source of this difference requires a brief summary of their work.

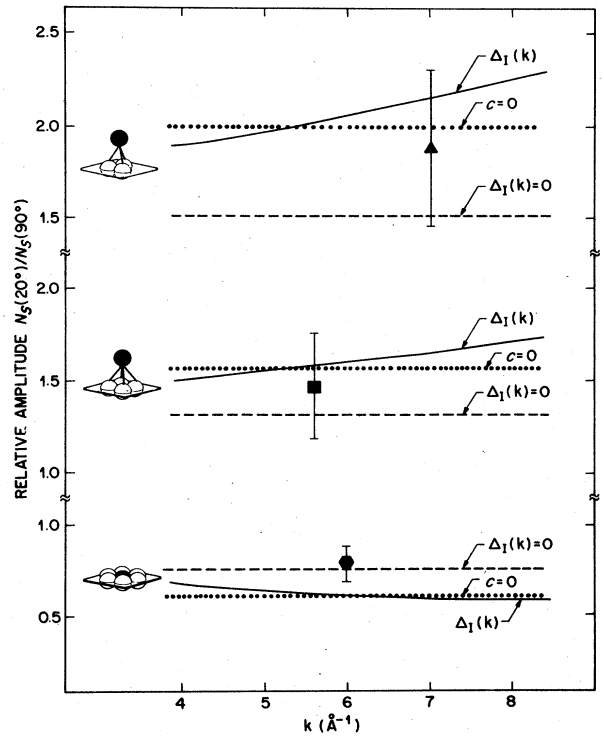

FIG. 12. Comparison between experimental SEXAFS amplitude ratios, indicated by geometric shapes with error bars, and the predictions of Eq. (25) using (i) calculated values of $\Delta_I(k)$ (Ref. 25), (ii) $\Delta_I(k)=0$, and (iii) $c=0$. The k-averaged experimental relative amplitudes are shown at some intermediate value of k. For I-Cu(111) and I-Cu(100) (Ref. 11), top and middle cases, it is not possible to distinguish between conditions (i), (ii), and (iii). For Te-Cu(111) (Ref. 15), bottom case, only the approximation labeled $\Delta_I(k)$ [$\approx\Delta_{Te}(k)$] is consistent with experiment.

Stöhr *et al.* measured L_2-edge SEXAFS from Ag on Si(111) as a function of coverage and temperature. At coverages above 1 monolayer (ML), clear evidence for clustering of Ag metal was found, which was characterized by a Ag-Ag peak in the Fourier-transformed SEXAFS data at ~ 2.8 Å and an approximately 50% smaller satellite at ~ 2.0 Å due to a resonance in the Ag backscattering amplitude.[8,9] At Ag coverages below 1 ML a Ag-Si peak, also at ~ 2.0 Å, was observed to increase in intensity. The lowest coverages studied were 0.33 and 0.6 ML, and corresponded to unannealed and annealed samples, respectively. The quoted experimental relative amplitudes $N_S(90°)/N_S(25°)$ from these two samples, 1.45 ± 0.25 and 1.65 ± 0.15, were compared with those values calculated from Eq. (16) using either $c=0$ or $\Delta_{Ag}(k)=0$.[37] From this comparison two adsorption sites for Ag atoms were identified,[36] the threefold fcc hollow on top of the Si(111) surface for the 0.33 ML system and the sixfold quasicoplanar hollow (interstitial) between the first and second layers for the 0.6 ML system. Stöhr *et al.* argued that since the lowest calculated value for $N_S(90°)/N_S(25°)$ using $\Delta_{Ag}(k)=0$ is 1.47, which is outside the experimental value of 1.65 ± 0.15, the approximation of $\Delta_{Ag}(k)=0$ must be inappropriate. Because of this, and the fact that the calculated relative amplitudes are about equal at $k\sim 6$ Å^{-1} either assuming $c=0$ or using the TL-calculated value of $\Delta_{Ag}(k)$ in Eq. (16), Stöhr *et al.* analyzed the Ag-Si(111) data using the approximation of $c=0$.

The reason Stöhr *et al.* looked primarily at low coverage data was to minimize the contribution of Ag metal clusters. However, the 0.33 and 0.6 ML data contain Fourier peaks between 2.8—3.0 Å whose intensities are comparable to or greater than features originating from higher-frequency noise.[44] A narrow window function around the main peak (1.4—2.6 Å) cannot remove the contributing peaks in this region due to noise or to the Ag satellite at ~ 2.0 Å (should small amounts of Ag metal be present). Both of these effects therefore necessitate more realistic relative amplitude error limits of at least ± 0.25—0.3, particularly for the 0.6 ML system. This removes much of the apparent inconsistency between the value of 1.47 predicted with $\Delta_{Ag}(k)=0$ and the experimental value of 1.65. (The presence of Ag clusters would,

in fact, lead to a larger observed value.) It also demonstrates that like the threefold and fourfold hollow geometries in Figs. 11 and 12, the quasicoplanar geometry is not well suited for assessing the detailed nature of the cross term.

As mentioned in Sec. III B 1, the agreement between the average relative amplitude using the approximation of $c=0$ and that using the TL-calculated value of $\Delta_{Ag}(k)$ is a result of $\Delta_{Ag}(k\sim 6)$ being close to $-\pi/2$. However, since the calculated $\Delta_a(k)$ has been shown above to be inaccurate for I (Fig. 9) and since $\Delta_{Ag}(k)$ is essentially identical to $\Delta_I(k)$, not much significance can be attached to this agreement. In the absence of experimental evidence demonstrating that the calculated $\Delta_a(k)$ is indeed accurate, analysis of $L_{2,3}$-edge SEXAFS data using $c=0$ can only be assumed valid for systems with β or θ values near the central unshaded region in Fig. 8. The simple approximation of $\Delta_a(k)\approx 0$, on the other hand, has been empirically shown above and in Ref. 14 to be reliable in the analysis of I $L_{2,3}$-edge SEXAFS data even for the worse-case condition of the atop geometry. The similarity between $\Delta_I(k)$ and $\Delta_{Ag}(k)$, and the fact that the inaccuracies in the calculated central-atom phase shifts for I are likely to be present for Ag as well,[41] suggest that the approximation $\Delta_a(k)\approx 0$ should also be applicable to Ag.

Bond-length anisotropies due to the cross term were also stated to be present in the data of Stöhr *et al.* They quote Ag-Si bond lengths of 2.48 ± 0.04 Å and 2.46 ± 0.04 Å in the 0.6 ML system measured at $\theta=90°$ and 25°, respectively. The 0.02-Å shorter bond length at $\theta=25°$ agrees with the corresponding shortening of 0.03 Å determined from their analysis of Ag-Si simulated data.[36] However, it was shown in Sec. III B 1 that their analysis of simulated data[21,36] overestimates the determination of bond-length errors due to the cross term. Using different analysis procedures described in that section and elsewhere,[8] the simulated Ag-Si data for the configuration in question is found here to give an error of only 0.011 Å. This value is also consistent with the bond-length anisotropy of $\lesssim 0.01$ Å observed[15] for the case of Te on Cu(111), which has almost the same configuration as that proposed for the 0.6-ML Ag-Si(111) system.

The above considerations can be generalized to the following conclusions. Bond-length anisotropies (not total errors[45]) due to the effects of the cross term are largest for atoms in the atop geometry, $\lesssim 0.02$ Å, next largest for the coplanar geometry <0.015 Å, and less than 0.01 Å for all others. The essential constancy of the calculated $\Delta_a(k)$ values for all atoms (see next section) and the fact that the effect of the calculated $\Delta_a(k)$ values on the phase is a maximum (see Fig. 1) makes this statement generally valid under all conditions. With regard to relative amplitudes, the differences predicted from simulated data as a result of using $c=0$, $\Delta_a(k)=0$, or $\Delta_a(k)\neq 0$ in Eq. (16) are possible to distinguish experimentally for atoms in the atop geometry. For other geometries, realistic experimental uncertainties make it more difficult to distinguish between these conditions. This is particularly so since the inherent uncertainties in the calculated values of $\Delta_a(k)$, which have thus far been ignored, must be taken into account. Correcting the calculated curves labeled $\Delta_I(k)$ in Fig. 12 as was done in Fig. 10, for example, makes it even more difficult to distinguish between them and those labeled $\Delta_I(k)=0$. The conclusion from these results, therefore, is that for the atoms I and Te (and probably Ag) the approximation of $\Delta_a(k)=0$ should be valid for determining average relative amplitudes from $L_{2,3}$-edge SEXAFS data for any adsorption geometry (other atoms are considered in the next section). The approximation $c=0$, on the other hand, is not valid for these atoms because it neglects the inaccuracies of the calculated $\Delta_a(k)$ values.

D. General analysis of $L_{2,3}$-edge data

The preceding section has shown that with the exception of the atop geometry, the atoms Ag, Te, or I in other adsorption geometries do not exhibit dramatic effects due to the cross term in their $L_{2,3}$-edge SEXAFS. That is, strong modifications in either the SEXAFS bond lengths or relative amplitudes as a result of $\Delta_a(k)$ being finite *or* zero are difficult to observe in these other geometries, and for these atoms the simplifying approximation of $\Delta_a(k)=0$ appears to be valid. The question arises as to how well this result can be generalized to other atoms. In Fig. 13 the calculated[25] values of $\Delta_a(k)$ are plotted for a range of elements. Despite the fact that the individual central-atom phase shifts $\phi_a^{l=2}(k)$ and $\phi_a^{l=0}(k)$ for these elements are very different, their differences [Eq. (8)] are remarkably similar. Thus, *if* these calculated $\Delta_a(k)$ values were accurate, analysis of their average $L_{2,3}$-edge SEXAFS amplitudes could be well approximated assuming $c=0$ for *any* atom because *all* of the values of $\Delta_a(k\sim 6)\approx -\pi/2$ (see Sec. III B 1). However, short of a direct empirical test as was done for I in Sec. III B 2, it is not possible to assess the inaccuracy of the $\Delta_a(k)$ values for the other elements. For example, instead of the positive correction to $\Delta_a(k)$ needed for I (see Figs. 9 and 10), a zero or even negative correction may be needed for a different element. With a correction of any magnitude or sign to the calculated $\Delta_a(k)$ value, its effect on the total phase would always be reduced because Δ_a ($k\sim 6$–7), and

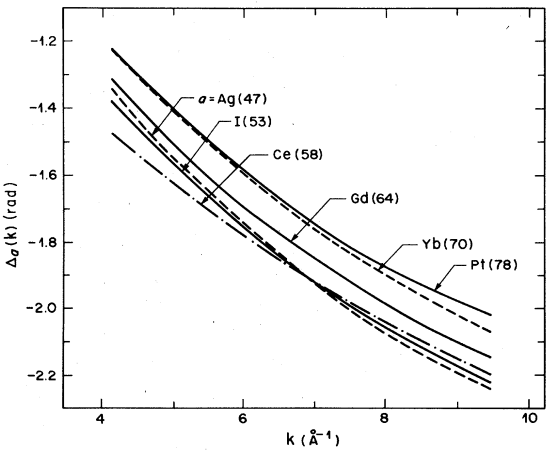

FIG. 13. Calculated values of $\Delta_a(k)$ [Eq. (10)] from Ref. 25 as a function of absorbing atom a. Despite the very different individual $\phi_a^{l=0}(k)$ and $\phi_a^{l=2}(k)$ values, their difference is nearly constant for all elements.

thus $\psi(\theta)$, is a maximum, see Fig. 1.[46] With regard to the relative amplitude, however, a negative correction to $\Delta_a(k)$ would actually increase its effect. Thus, while the preceding section did establish that a finite $\Delta_a(k)$ is of less importance for adsorption geometries other than the atop configuration, a value of $\Delta_a(k)$ more negative than the calculated one could be potentially more important on the amplitude. What is needed, therefore, is a general procedure for determining adsorption geometries and bond lengths from $L_{2,3}$-edge SEXAFS data which is independent of any assumptions about the accuracy of the calculated $\Delta_a(k)$ values. A simple empirical approach for doing this is presented below.

One way to remove the effect of the cross term in the $L_{2,3}$-edge absorption from an anisotropic surface system is to make the SEXAFS measurement at $\theta=54.7°$, the angle at which $3\sum_i^N |\hat{\epsilon}\cdot\hat{r}_i|^2=N$. The SEXAFS values of R and N referenced with respect to either simulated data or, preferably, data from a model compound, then reflect the actual bond length and coordination number. If only a single SEXAFS measurement is made, however, possible systematic errors due to sample imperfections or coverage inhomogeneities, for example, may not be detected. Furthermore, any polarization dependence of the measured distance which could arise from anisotropic averaging of different neighbor contributions (see below) will also go undetected. An alternate approach for removing the effects of the cross term is to make two different measurements from the same system at normal ($\theta=90°$) and grazing ($\theta\lesssim 25°$) photon incidence angles, and then take linear combinations of the data as described in Sec. III B 2, see Eq. (28). As with a single measurement at $\theta=54.7°$, a direct determination of R is obtained, i.e., no modifications due to $\Delta_a(k)$ need be considered. However, in addition to providing an important consistency check for systematics and testing for polarization-dependent distances, there is another factor to consider. The values of the absolute amplitudes of the *linearly combined* data, i.e., N^* in Eq. (28), are larger than the values of N derived from the individual data, and these make it easier to distinguish between various adsorption sites.

As examples of how the adsorption geometry can be determined using these general procedures, consider the case of an atom adsorbed on a Cu(111) and a Si(111) surface. The former is treated first. The relatively larger second-nearest-neighbor distances in Cu(111) lead to only first-neighbor Cu atoms dominating the measured SEXAFS. A first-neighbor adsorbate-Cu distance $R_1=2.5$ Å is assumed. The highest-symmetry adsorption sites are indicated in Fig. 14(a) and are given the notation A for atop, B for bridge, F for fcc hollow (i.e., with no Cu atom lying directly below in the second layer), H for hcp hollow, and S for substitutional [i.e., within the Cu(111) surface]. The values of N for these sites are 1,2,3,3, and 6, respectively. In addition to N, two other quantities are shown in Fig. 14(a), $N^*=n_d(20°)-[n_{sd}(20°)/n_{sd}(90°)]n_d(90°)$, from Eq. (28), and the relative amplitude $N_S(20°)/N_S(90°)$, calculated assuming $\Delta_a(k)=0$. (For the purposes of this discussion it is not necessary to assume that $\Delta_a(k)=0$, but the assumption of $c=0$ [which is a reasonable approximation for those elements whose calculated $\Delta_a(k)$ values may be accurate] does not alter the conclusions below and only makes the differences in relative amplitudes even greater for the different sites.) Inspection of N, N^*, and $N_S(20°)/N_S(90°)$ shows that sites A and S can be easily distinguished from a measurement of relative amplitudes alone, but that such quantities are insufficiently different to distinguish between sites B and (F,H) (the difference between F and H for these and other close-packed systems is not possible to determine with SEXAFS). It is this result, i.e., that $L_{2,3}$-edge SEXAFS

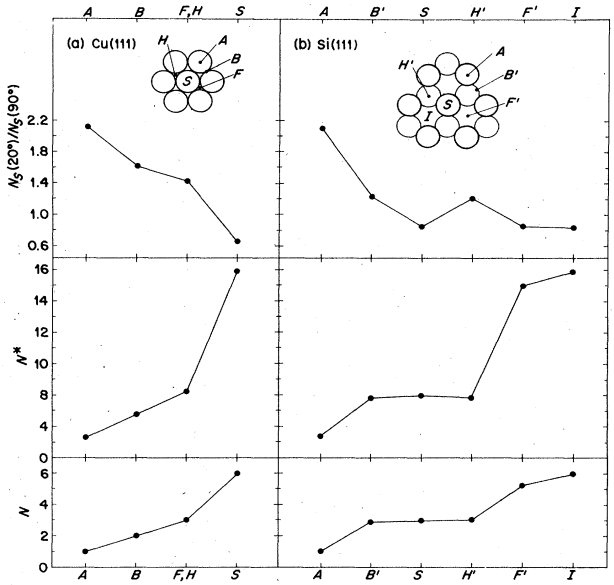

FIG. 14. Predicted values of absolute and relative coordination numbers as a function of high-symmetry adsorption site for the case of an atom absorbed on a (a) Cu(111) and (b) Si(111) surface. An adatom in the atop (A), bridge (B), fcc hollow (F), or hcp hollow (H) site lies above the surface, in the substitutional (S) site it is within the surface, and in the interstitial (I) site in (b) it is below the surface between the first and second layers. The prime notation in (b) indicates that the closely spaced second-neighbor atoms can contribute to the measured SEXAFS. The effect of the s-d cross term is approximated by setting $\Delta_a(k)=0$ (adsorption site assignments are not strongly affected by this approximation). The effect of the second-neighbor contributions is assumed to be zero in (a) with $R_1=2.50$ Å, in (b) it is approximated by using Eq. (32) and the R_1 and R_2 values from Ref. 36 (these are listed in parentheses in Table IV). N^* is calculated from Eq. (28) and N is calculated from $\overline{N}_S(\theta)$ [Eq. (32)] with $\theta=54.7°$. The lines connecting the different values serve only as a visual guide. In (a) it is possible to identify sites A and S using the relative amplitudes, while for site B and sites F or H (which are indistinguishable in SEXAFS) the absolute amplitude N is required. Using the quantity N^* the adsorption sites can be distinguished from even simulated data (relative amplitudes should nonetheless be obtained to minimize systematic errors). In (b), sites A, S and I can be identified as in (a), while sites B', H', and F' require considering the contribution from the second-neighbor atoms. This can be accomplished from a study of both the SEXAFS amplitudes and the polarization-dependent distances [Eqs. (31) and (32) are simplifying approximations; Eq. (36), used in Fig. 15, is more exact].

measurements of effective coordination numbers for certain sites are too similar, which is responsible for the fact that *both* absolute and relative amplitudes are generally necessary for a reliable determination of adsorption site geometries.[11,14,15] From Fig. 14(a) it is easy to see that the absolute coordination numbers provide the necessary information for distinguishing between the different adsorption sites. What has not been previously appreciated is that this statement applies *even if a model compound is not available.* The difference in N^* for sites B and (F,H), i.e., 5.45 versus 8.39, is large enough to allow even *simulated* SEXAFS data to be used with confidence. Knowledge of the actual adsorption site is not needed *a priori* despite the fact that this information goes into the calculation of the corresponding values of $n_{sd}(20°)$ and $n_{sd}(90°)$ which comprise N^* in Eq. (28). The reason for this is that the ratio $n_{sd}(20°)/n_{sd}(90°)$ or $n_{sd}(\theta_1)/n_{sd}(\theta_2)$, in general, is nearly *constant* for all adsorption sites, see Table III. Thus, for example, if the $n_{sd}(20°)/n_{sd}(90°)$ ratio for the fcc hollow site were incorrectly applied to a data representative of an adatom in the bridge site, the value of N^* would be 5.61 instead of 5.45, a negligible error. By the same token, using Eq. (28) and an average value of $n_{sd}(\theta_1)/n_{sd}(\theta_2)$ provides a very accurate determination of R irrespective from knowing the adsorption site. With this procedure, the accuracy of R will always be limited by the uncertainty of R_M in the model system, just as in the case of K-edge data.

Consider now an atom adsorbed on a Si(111) surface. For an ideal Si(111)1×1 surface the first- and second-layer Si atoms are separated by only 0.78 Å, so the second-neighbor contributions for certain sites cannot be ignored. The high-symmetry sites for Si(111) are indicated in Fig. 14(b), with a notation analogous to that used in Fig. 14(a). An additional site labeled I for interstitial has been indicated, lying midway between the first and second Si(111) layers. The degree to which the second-neighbor Si atoms contribute SEXAFS relative to that from the first-neighbor atoms depends on the distances R_1 and R_2. Table IV lists the values of R_2 as a function of site using $R_1=2.50$ Å. Since this R_1 distance is also close to the sum of covalent radii for Ag and Si (2.51 Å) it can be considered representative of the Ag-Si(111) system. For comparison, values of R_1 and R_2 assumed in Ref. 36 for the Ag-Si distances in Ag-Si(111) are shown in parentheses. Sites A, S, and I are seen to have ΔR $(=R_2-R_1)$ values $\gtrsim 1.5$ Å, large enough for standard Fourier filtering procedures to isolate the second-neighbor shell contribution (see, e.g., Fig. 5). Sites B', H', and F', on the other hand, have much smaller ΔR values, making such procedures useless for shell separation. The prime notation has thus been used to indicate that second-nearest-neighbor atom contributions are possible for these sites.

TABLE III. Values of $n_{sd}(20°)/n_{sd}(90°)$ for different adsorption geometries.

System	Site[a]	$n_{sd}(20°)/n_{sd}(90°)$
Cu(111)	A	−1.65
	B	−1.84
	F,H	−1.73
	S	−1.65
Si(111)	A	−1.65
	B'	−1.64
	S	−1.65
	H'	−1.57
	F'	−1.84
	I	−1.65

[a]See text and Fig. 14 for description of sites.

The identification and characterization of an adatom in one of the unprimed sites A, S, or I on Si(111) are the same as for the case of an adatom on Cu(111). Thus, for example, the quoted value[14] for R in I-Si(111) was determined from Eq. (28) using the calculated quantity $n_{sd}(90°)/n_{sd}(35°)=-1.01$ [note that in this example an equivalent result is obtained by simply taking the mean value of $R(35°)$ and $R(90°)$, see Sec. III B 2]. Similarly, the distinction between sites A, S, and I for Si(111) can be readily accomplished using relative and absolute amplitudes N or N^*. Model compounds are unnecessary. Figure 14(b) shows the values of N, N^*, and $N_S(20°)/N_S(90°)$ for these three sites calculated using $R_1=2.48$ Å from Stöhr *et al.*[36] These authors state in their analysis of Ag on Si(111) that site S could not be distinguished from site I due to the unavailability of a Ag-Si model compound. However, the distinction between the very different $N^*(N)$ values of 7.96(3.0) and 15.9(6.0) from Fig. 14(b) could be performed using simulated date since the uncertanties in the theoretical amplitudes[25] are much smaller than these large differences.

For an adatom in one of the primed sites B', H', and F' on Si(111), different analysis procedures are required. The simplest approach for incorporating the effects of the second-neighbor shell of Si atoms is to assume an arithmetic sum of first and second shells.[14,36] The total $L_{2,3}$-edge SEXAFS obtained with this assumption is analogous

TABLE IV. Second-neighbor Ag-Si distances for Ag on Si(111) [where an ideal Si(111)1×1 surface is assumed] as a function of first-neighbor distance and adsorption site [see text and Fig. 14b) for description of adsorption sites]. The values of $R_1=2.50$ Å corresponds closely to the sum of Ag-Si covalent radii (2.51 Å); the values of R_1 and R_2 in parentheses are from Ref. 36.

	A	B'	S	H'	F'	I[a,b]
R_1	2.50(2.48)	2.50(2.48)	2.50(2.48)	2.50(2.13)	2.50(2.34)	2.50(2.48)
R_2	3.96(3.95)	2.63(2.60)	4.01(4.00)	2.80(2.60)	2.95(2.70)	4.01(4.00)
ΔR	1.46(1.47)	0.13(0.12)	1.51(1.52)	0.30(0.47)	0.45(0.36)	1.51(1.52)

[a]For Ag (or any atom) in the interstitial site I with R_1 greater than 2.35 Å (the Si-Si nearest-neighbor distance), an expansion of the Si double-layer distance is required.

[b]No lateral rearrangements are assumed here, while Ref. 36 did assume small lateral rearrangements.

to Eq. (24),

$$\chi(k,\theta)\approx A'(k)\bar{N}_S(\theta)\sin[2k\bar{R}(\theta)+\phi_{2b}(k)+\psi(k,\theta)] . \tag{31}$$

The average effective coordination number is

$$\bar{N}_S(\theta)=N_{S1}(\theta)+(R_1/R_2)^2N_{S2}(\theta) , \tag{32}$$

with the individual values of $N_{S1}(\theta)$ and $N_{S2}(\theta)$ being described by Eq. (25). The measured distances are polarization-dependent weighted averages,

$$\bar{R}(\theta)=\{N_{S1}(\theta)R_1+[\bar{N}_S(\theta)-N_{S1}(\theta)]R_2\}/\bar{N}_S(\theta)$$
$$=[R_1+a(\theta)R_2]/[1+a(\theta)] , \tag{33}$$

where

$$a(\theta)=(R_1/R_2)^2N_{S2}(\theta)/N_{S1}(\theta) . \tag{34}$$

In Fig. 14(b) the values of N, N^*, and $N_S(20°)/N_S(90°)$ have been indicated for sites B', H', and F' using Eqs. (31) and (32). From this figure it appears that site S can be readily distinguished from sites B' and H' using relative amplitudes (the absolute amplitudes are nearly identical). Discriminating between sites B' and H' or F' and I, on the other hand, appears difficult even using both relative and amplitude amplitudes. One approach to this problem is to analyze the polarization dependence of $R(\theta)$ (i.e., the relative distances) according to Eq. (33) and to compare the absolute values of $R(\theta)$ with expected values of R_1. Such considerations of absolute and relative distances have been carried out in previous studies[14] and shown to give qualitatively useful information. It will now be shown that by using a more accurate description of the interference between the SEXAFS from two different coordination shells it is even more straightforward to discriminate between various adsorption sites.

Equations (31) and (32) are valid so long as $\Delta R \ll 1$, but they break down dramatically as ΔR increases. The reason for this is identical to why the effect of the total cross term depends so strongly on the value of $\Delta_a(k)$, namely, the interference between two circular functions depends not only on their relative amplitudes but also very sensitively on the difference of their phases. The expression for the total $L_{2,3}$-edge SEXAFS from two shells composed of the same atoms at R_1 and R_2 is actually given by

$$\chi(k,\theta)=A_1'(k)N_{S1}(\theta)\sin[2kR_1+\phi_{2b}(k)+\psi_1(k,\theta)]$$
$$+A_2'(k)N_{S2}\sin[2kR_2+\phi_{2b}(k)$$
$$+\psi_2(k,\theta)], \quad L_{2,3} \text{ edges} . \tag{35}$$

An analogous expression for K-edge SEXAFS can be written using $[2kR_j+\phi_{1b}(k)]$ for the phase and $N_{S_j}(\theta)$ defined by Eq. (4). For isotropic EXAFS from $L_{2,3}$ or K edges, $N_{S_j}(\theta)=N_j$. (The situation of isotropic K-edge absorption for two closely spaced shells has been previously considered by Martens *et al.*[47]) Assuming for simplicity[48] that $A_2'(k)=(R_1/R_2)^2A_1'(k)$ and defining $\Delta\psi(k,\theta)=\psi_2(k,\theta)-\psi_1(k,\theta)$, Eq. (34) can be rewritten [see Eqs. (21)–(23)] as

$$\chi(k,\theta)=A_1'(k)N_{S1}(\theta)\mathscr{A}(k,\theta)$$
$$\times\sin[2k\bar{R}(\theta)+\phi_{2b}(k)+\Psi(k,\theta)] , \tag{36}$$

where

$$\mathscr{A}(k,\theta)=(\{1+a(\theta)\cos[2k\Delta R+\Delta\psi(k,\theta)]\}^2$$
$$+a^2(\theta)\sin^2[2k\Delta R+\Delta\psi(k,\theta)])^{1/2} , \tag{37}$$

$$\Psi(k,\theta)=2ka(\theta)[\bar{R}(\theta)-R_2]+\psi_1(k,\theta)+\Gamma(k,\theta) , \tag{38}$$

$$\Gamma(k,\theta)=\tan^{-1}\left[\frac{a(\theta)\sin[2k\Delta R+\Delta\psi(k,\theta)]}{1+a(\theta)\cos[2k\Delta R+\Delta\psi(k,\theta)]}\right] . \tag{39}$$

Only when ΔR is $\ll 1$ will the second term in Eq. (38) [due mainly to $\Delta_a(k)$] be comparable to the first and third terms (due mainly to ΔR), because ΔR is multiplied by $2k$. The polarization dependence of the total SEXAFS phase will thus be determined primarily by the magnitude of ΔR. Even more significant than the effect of ΔR on the total phase is the extremely large effect of ΔR on the total SEXAFS amplitude. To see this by inspection, consider the limiting case when $a(\theta)=1$, whereupon $\bar{R}(\theta)=[R_1(\theta)+R_2(\theta)]/2$, $\Psi(k,\theta)=[\psi_1,(k,\theta)+\psi_2(k,\theta)]/2$, and $\mathscr{A}(k)=2\cos[k\Delta R+\Delta\psi(k,\theta)/2]$. Under the condition when $(k\Delta R+\Delta\psi(k,\theta)/2)=\pi/2$ the total SEXAFS amplitude becomes *zero*. Taking $\Delta R=0.36$ Å, for example, and neglecting $\Delta\psi(k,\theta)/2$ (it is $\ll k\Delta R$), the total SEXAFS amplitude becomes zero at $k=4.4$ Å^{-1}. The other extreme occurs at $k=8.8$ Å^{-1}, where $\mathscr{A}(8.8)=-2$. Thus when $a(\theta)=1$ the breakdown of Eqs. (31) and (32) for even modest values of ΔR is seen to be substantial. As $a(\theta)$ becomes smaller than 1, of course, the effect of ΔR decreases.

The above discussion points out the competition between three terms: ΔR, $a(\theta)$, and $\Delta_a(k)$. To illustrate their relative importance more graphically, simulated Ag-Si(111) data were generated from Eq. (36) for Ag occupying sites B', H', and F' on an ideal Si(111)1×1 surface using the R_1 and R_2 values assumed in Ref. 36 (see Table IV), values of $a(\theta)$ according to Eq. (34), and the calculated $\Delta_{Ag}(k)$ value from Ref. 25. The results are shown in Fig. 15 for $\theta=20°$ (solid lines) and $\theta=90°$ (dashed lines). Almost identical spectra were obtained using $\Delta_{Ag}(k)=0$ (not shown), confirming that the effect of ΔR is much larger than that of $\Delta_{Ag}(k)$ due to the multiplicative factor of $2k$ (also see below). For comparison, the simulated Ag-Si(111) SEXAFS for Ag in sites A, S, and I [and with $\Delta_{Ag}(k)$ from Ref. 25] are shown in Fig. 15. Superposed on all these spectra with a dotted line is the simulated EXAFS data from the hypothetical model compound $AgSi_3$ ($R_{Ag\text{-}Si}=2.5$ Å). The distinction between all the sites is clearly apparent. The spectra for sites B' ($\Delta R=0.12$ Å) and H' ($\Delta R=0.47$ Å) not only have different polarization-dependent distances and different total phases, but the total amplitude of the spectrum for site H' is significantly altered with respect to that of B' (or $AgSi_3$). Distinguishing between sites F' ($\Delta R=0.36$ Å) and I ($\Delta R=0$) is also not difficult. The polarization dependence of $R(\theta)$ for site F' due to the effect of ΔR is greater than and of opposite sign to that for site I due to the effect of $\Delta_{Ag}(k)$. More obvious, however,

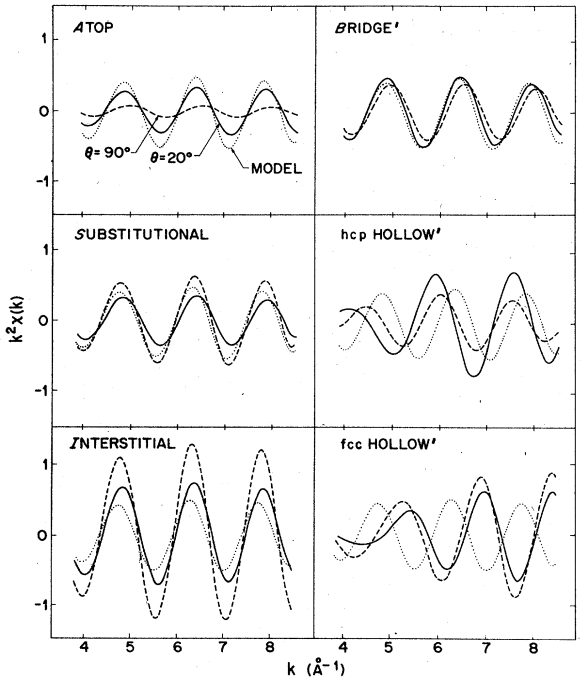

FIG. 15. Simulated $L_{2,3}$-edge data for Ag occupying different adsorption sites on a Si(111)1×1 surface. The effect of the cross term is treated by using the calculated value of $\Delta_{Ag}(k)$ from Ref. 25 (as in Fig. 14, this is unimportant), while the effect of the second-neighbor contributions is treated more exactly by using Eq. (36). The values of R_1 and R_2 from Ref. 36 are used. Simulated data from the hypothetical model compound Ag_3Si with $R_1=2.50$ Å are indicated by the dotted line. Note the very large differences in polarization-dependent distances, absolute amplitudes, and overall displacements between the different sites.

are the very different amplitudes, with that of F' being not only smaller in magnitude but almost completely *antiphase*.[49] This situation is reminiscent of the one considered above for $\Delta R=0.36$ Å and $a(\theta)=1$.

The effects of ΔR versus $\Delta_a(k)$ as a function of adsorption site can be quantified. Table V summarizes the values of $R_{Ag\text{-}Si}(\theta)$ for $\theta=20°$ and 90° evaluated with two different procedures. The first, labeled I, approximates the interference between the first- and second-atom shells using Eq. (31) and approximates the interference between the s and d final states by setting $\Delta_{Ag}(k)=0$, i.e., Eq. (20). The second, labeled II, determines $R_{Ag\text{-}Si}(\theta)$ from analysis of simulated data using the more exact interference expression, Eq. (35), and the calculated value[25] of $\Delta_{Ag}(k)$, i.e., Eq. (25). Both methods use the values of R_1 and R_2 assumed in Ref. 36. Because the total amplitudes for the spectra of sites H' and F' are so different using method II from that of the model system (see Fig. 15), standard analysis procedures could not be applied and analytical treatment of the simulated data was necessary to evaluate $R(\theta)$ (the quantities N and N^* for these sites are not meaningful). Comparison between the values of $R(\theta)$ determined from methods I and II show that their differences are only quantitative. Thus if the interference effects between the first- and second-atom shells were only approximated (as in method I) but the interference effects due to a finite[25] $\Delta_a(k)$ were included (as in method II), the net effect on the distances would be comparable to or smaller than the differences seen in Table V. The difficulty in obtaining quantitative values of R_1 and R_2 for sites B', H', and F' is a general one in both K-edge and $L_{2,3}$-edge SEXAFS and EXAFS data. However, the explicit consideration of the competition between the effects from ΔR and $\Delta_a(k)$ in the case of Ag on Si(111) is system dependent since it varies with both the values of ΔR (Ref. 36) and the calculated value of $\Delta_{Ag}(k)$.[25] Its purpose is to show how in this system the effects of ΔR dominate due to the multiplicative $2k$ term and the comparatively small effect of $\Delta_{Ag}(k)$ for the other adsorption geometries.[49]

Summarizing this section, general procedures for removing the effects of the cross term and for reliably determining bond lengths and adsorption sites from $L_{2,3}$-edge SEXAFS data have been described. The use of a model compound is still valuable for providing the most accurate determination of R, but to distinguish between high-symmetry adsorption sites these general procedures can rely on even simulated data. For the Cu(111) surface, for example, a measurement of both absolute and relative amplitudes alone is sufficient for identifying the adsorption site. This is also true for most of the sites on the Si(111) surface. However, for some of the sites on the Si(111) surface a measure of the polarization dependence of the distance is also required. The procedures developed for these surfaces are empirical and should be applicable to other systems.

IV. SUMMARY

The transition probability for $L_{2,3}$-edge absorption contains three terms corresponding to final states of s, d, and s-d symmetry. The first is negligible compared with the

TABLE V. Ag-Si distances for Ag on Si(111) as a function of adsorption site [see text and Fig. 14(b) for description of sites] and method of determination. Method I uses Eq. (31) with $\psi(k,\theta)=0$, i.e., the interference effects from both the different first- and second-neighbor atom shells and from the s-d cross term are only approximated; method II uses Eq. (35) with $\Delta_{Ag}(k)$ from Ref. 25, i.e., both interference effects are included explicitly. Values of R_1 and R_2 assumed in Ref. 36 are used here (see Table IV). (Some of the distances in this table using method I are slightly different from those in Ref. 36 using the same method due, in part, to the use of $\theta=20°$ rather than 25°.)

	A		*B'*		*S*		*H'*		*F'*		*I*	
	I	II	I	II	I	II	I	II	I	II	I	II
$R(20°)$	2.48	2.48	2.48	2.48	2.48	2.47	2.39	2.43	2.51	2.50	2.48	2.47
$R(90°)$	2.48	2.46	2.47	2.45	2.48	2.48	2.48	2.52	2.49	2.46	2.48	2.48

second while the third is zero for isotropic absorbers. For the case of anisotropically distributed adatoms on a single-crystal surface, the contribution of the s-d cross term is nonzero and must be included with the transition probability of the d state. The result of doing this has been a subject of recent discussion. If the SEXAFS associated with the adatom's outgoing s-state photoelectron wave is in phase (or very nearly so) with that of the d-state wave, then the s-d and d absorption terms simply add and only the SEXAFS amplitude is modified. If, on the other hand, the s and d waves are sufficiently out of phase, then the two interfere and both the SEXAFS amplitude and phase are affected. Based on generally accepted calculated phase shifts[25] for s and d waves and using the Ag adatom as an example, simulated SEXAFS data had been analyzed and shown that it was the latter situation which was the case.[21] In particular, for the configuration of Ag in the atop site, that analysis gave a bond-length anisotropy of ~ 0.05 Å and an amplitude correction of about a factor of 2. A comparable bond-length anisotropy and an amplitude correction of ~ 1.5 were obtained for Ag in a coplanar geometry. The conclusion[21] that effects of such large magnitude are a general phenomenon and the fact that these predictions are at odds with both the analysis and the experimental data from previous I and Te $L_{2,3}$-edge SEXAFS work[11,14,15] motivated the present study.

First, the validity of the predictions regarding the effects of the s-d cross term in the simulated data was checked using the example of I in the atop configuration. The very large modification of the SEXAFS amplitude was confirmed, but the effect on the determined bond length was shown to be overestimated by a factor of 2 as a result of the particular method used[21] in the data analysis. The predictions based on the simulated data were then compared with the experimental data of I in the atop configuration. Evidence for the small bond-length anisotropy could be identified (a value of ~ 0.02 Å, or a bond-length imprecision from this effect of ± 0.01 Å), but the sizable amplitude corrections were decidedly absent. Using two different empirical procedures the source of this discrepancy for I was traced to the inaccuracy of the calculated phase shifts involved in generating the simulated data. It was shown that the actual relative phase between the s- and the d-state waves, a quantity defined as $\Delta(k)$, is about half the theoretical value.[25] This result demonstrates why the effect of the s-d cross term on the SEXAFS amplitude is well approximated by its simple addition to the d-absorption term as had been performed in the initial studies.[11,14,15] It further shows that while calculated phase shifts may be useful for obtaining qualitatively accurate bond lengths from EXAFS data, their strong effect on the interference between the s-d and d-state terms places unrealistic demands on their accuracy required for meaningful analysis of SEXAFS data.

The above result carries with it a number of implications which depend on three factors: the type of absorbing (*ad*)atom, the configuration of that atom with respect to the surface, and the accuracy of the calculated relative phase shifts for that atom, i.e., the accuracy of $\Delta(k)$. The first factor was examined by assuming the calculated $\Delta(k)$ values to be accurate and comparing these values for different atoms. Within ± 0.1 rad they were all very similar, implying that conclusions based on simulated data alone should apply to any atom. The second factor was examined by again assuming accurate $\Delta(k)$ values and comparing simulated data for I or Te in different adsorption sites with corresponding experimental data. The goal was to study not only the importance of the s-d cross term as a function of adsorption site but also to see whether atoms in other sites could be used to assess the reliability of the calculated $\Delta(k)$ values. It was found that the atop configuration exhibits the greatest sensitivity to the effects of s-d cross term and so is the best suited for empirically determining $\Delta(k)$. For SEXAFS data with less than very high signal-to-noise quality it was shown that it is difficult to evaluate $\Delta(k)$ for atoms in other adsorption geometries, including the coplanar configuration.

The accuracy of $\Delta(k)$, the third factor, affects the above conclusions regarding different atoms and different adsorption sites because these are all based on simulated data generated from calculated $\Delta(k)$ values. Since it was shown that $\Delta(k)$ is, in fact, not accurate for I (and undoubtedly for nearby elements such as Te and Ag), it is tempting to assume that the same corrections to $\Delta(k)$ apply for all atoms. However, without experimental evidence from a broader range of elements this assumption cannot be justified. A general procedure for analyzing $L_{2,3}$-edge SEXAFS data was therefore developed which eliminates the need for making any assumptions about $\Delta(k)$. Using this empirical procedure it is possible to determine bond lengths and adsorption sites with a reliability comparable to that obtainable from K-edge SEXAFS data.

ACKNOWLEDGMENTS

The author thanks B. M. Kincaid for several helpful discussions and B. Buntschuh for his skillful assistance with the simulated data.

[1]R. de L. Kronig, Z. Phys. **70**, 317 (1931); **75**, 468 (1932).
[2]E. A. Stern, Contemp. Phys. **19**, 289 (1978).
[3]P. Eisenberger and B. M. Kincaid, Science **200**, 1441 (1978).
[4]D. R. Sandstrom and F. W. Lytle, Ann. Rev. Phys. Chem. **30**, 215 (1979).
[5]S. P. Cramer and K. O. Hodgson, in *Progress in Inorganic Chemistry*, edited by S. J. Lippard (Wiley, New York, 1979), Vol. 25, p. 1.
[6]B. K. Teo, Acc. Chem. Res. **13**, 412 (1980).
[7]P. Rabe and R. Haensel, in *Festkörperprobleme 20* (Pergamon-Vieweg, Stuttgart, 1980), p. 43.
[8]P. A. Lee, P. H. Citrin, P. Eisenberger, and B. M. Kincaid,

Rev. Mod. Phys. **53**, 769 (1981).
[9]P. H. Citrin, P. Eisenberger, and R. C. Hewitt, Phys. Rev. Lett. **41**, 309 (1978).
[10]L. I. Johansson and J. Stöhr, Phys. Rev. Lett. **43**, 1882 (1979); J. Stöhr, L. I. Johansson, S. Brennan, M. Hecht, and J. N. Miller, Phys. Rev. B **22**, 4052 (1980).
[11](a) P. H. Citrin, P. Eisenberger, and R. C. Hewitt, Phys. Rev. Lett. **45**, 1948 (1980); (b) **47**, 1567 (1981).
[12]Ordered bulk materials with less than cubic symmetry are obvious exceptions, e.g., single-crystal Zn, G. S. Brown, P. Eisenberger, and P. Schmidt, Solid State Commun. **24**, 201 (1977).
[13]S. Brennan, J. Stöhr, and R. Jaeger, Phys. Rev. B **24**, 4871 (1981).
[14]P. H. Citrin, P. Eisenberger, and J. E. Rowe, Phys. Rev. Lett. **48**, 802 (1982).
[15]F. Comin, P. H. Citrin, P. Eisenberger, and J. E. Rowe, Phys. Rev. B **26**, 7060 (1982).
[16]P. H. Citrin, D. R. Hamann, L. F. Mattheiss, and J. E. Rowe, Phys. Rev. Lett. **49**, 1712 (1982).
[17]J. Stöhr, R. Jaeger, and T. Kendelewicz, Phys. Rev. Lett. **49**, 142 (1982).
[18]P. H. Citrin, J. E. Rowe, and P. Eisenberger, Phys. Rev. B **28**, 2299 (1983).
[19]P. A. Lee and J. B. Pendry, Phys. Rev. B **15**, 2795 (1975).
[20]S. M. Heald and E. A. Stern, Phys. Rev. B **16**, 5549 (1977).
[21]J. Stöhr and R. Jaeger, Phys. Rev. B **27**, 5146 (1983).
[22]This expression is only approximate because multiple-scattering and many-body corrections to the amplitude are ignored. See, e.g., Ref. 8 for further details.
[23]More exact treatments of the vibrational and inelastic loss terms are not considered here. Derivations from the expressions in Eq. (3), e.g., due to anharmonic displacements, or apparent deviations due to static disorder can affect the determination of bond lengths and coordination numbers. See, e.g., Ref. 8.
[24]P. H. Citrin, P. Eisenberger, and B. M. Kincaid, Phys. Rev. Lett. **36**, 1346 (1976).
[25]B. K. Teo and P. A. Lee, J. Am. Chem. Soc. **101**, 2815 (1979).
[26]Deviations from these findings are small for $Z > 20$ and have a negligible effect on the conclusions of this paper.
[27]Equation (20) is different from that given in Ref. 11(b) by a factor of $\frac{3}{2}$ in order to make $\int N_S d\theta = N$.
[28]Because the possibility exists for small systematic errors (e.g., sample alignment or inhomogeneity) in SEXAFS measurements, determinations of both the absolute and relative amplitudes are important for establishing data reliability (see text later on).
[29]The I-Si(111) system is actually simple, despite the complex nature of the initially clean reconstructed Si(111)7×7 surface, because the I-Si chemisorption process saturates many of the dangling bonds (indirectly) involved in the 7×7 reconstruction.
[30]Values from Ref. 25 calculated from Herman-Skillman wave functions have been used here.
[31]SJ in Ref. 21 multiplied the simulated data by $f(\pi,k)/k$.
[32]Electron escape depths $\lambda(E)$ for kinetic energies $E > 100$ eV vary approximately as $\sqrt{E}$.
[33]M. B. Sterns, Phys. Rev. B **25**, 2382 (1982).
[34]B. A. Bunker and E. A. Stern, Phys. Rev. B **27**, 1017 (1983).
[35]G. Martens, P. Rabe, N. Schwentner, and A. Werner, Phys. Rev. B **17**, 1418 (1978).
[36]J. Stöhr, R. Jaeger, G. Rossi, T. Kendelewicz, and I. Lindau, Surf. Sci. **134**, 813 (1983).
[37]SJ (Ref. 21) and Stöhr *et al.* (Ref. 36) refer to the approximation "$\Delta_a(k)=0$" used here as "$c=0.2$."
[38]H. N. Rexroad, D. W. Howgate, R. C. Gunton, and J. F. Ollom, J. Chem. Phys. **24**, 625 (1956).
[39]The simulated data used values of $\theta=90°$ and 10°, rather than the experimental values of 90° and 35° (Ref. 14); this makes the theoretical bond-length anisotropy only somewhat larger.
[40]As noted in Ref. 33 there is clearly an error in the values of $\phi_{Ag}^{l=1}(k)$ published in Ref. 25. However, even after interpolation of adjacent values and using that phase shift in the analysis of the Ag L_1-edge data, substantial bond-length errors still remain.
[41]The observed errors in the calculated quantities $\Delta_l^*(k)$ and (see text below) $\Delta_l(k)$ are almost certainly due to uncertainties in the atomic potentials [P. A. Lee, private communication)]. Additional errors could also be introduced by the use of scattering plane waves rather than spherical waves, and this becomes increasingly important for high-Z atoms, cf., R. F. Pettifer and P. W. McMillan, Philos. Mag. **35**, 871 (1977). Such questions deserve consideration beyond the scope of this work.
[42]The fact that $\phi_a^{l=0}(k)$ and $\phi_a^{l=2}$ pertain to the same L_2 or L_3 edge means that any errors in E_0 disappear, but the possible uncertainties in the atomic potentials and in the use of plane waves (see Ref. 41) are still present.
[43]Unavoidable truncation errors, which are magnified in difference spectra, make the values of $\Delta_l(k)$ least reliable near the termination points.
[44]The signal-to-noise of the 0.6-ML Ag-Si(111) data from Ref. 36 is approximately half that of the 0.33-ML I-Cu(111) data from Ref. 11; that of the 0.33-ML Ag-Si(111) data is approximately one-fourth.
[45]Bond-length anisotropies refer to the maximum difference between $R(0°)$ and $R(90°)$ and should not be confused with bond-length errors, which are the differences between the actual value of R and the measured values of $R(\theta)$. Assuming two SEXAFS measurements are made at θ_1 and θ_2, for example, the average bond-length error (in the absence of the corrections described later on in the text) is just $R-[R(\theta_1)+R(\theta_2)]/2$, and this is always smaller than the corresponding bond-length anisotropy.
[46]SJ in Ref. 21 conclude on the basis of calculated $\Delta_a(k)$ values that the anisotropy in R due to the cross term will be enhanced in future SEXAFS data because they will extend to higher k values. As seen in Fig. 1(b), however, this statement is incorrect since the effect of $\Delta_a(k)$ on $\psi(k,\theta)$ decreases with increasing k.
[47]G. Martens, P. Rabe, N. Schwentner, and A. Werner, Phys. Rev. Lett. **39**, 1411 (1977).
[48]There can be differences in σ_2 and $\lambda_2(k)$ from σ_1 and $\lambda_1(k)$ which make $A_2'(k) < A_1'(k)$.
[49]The unannealed 0.33-ML Ag-Si(111) system in Ref. 36 was interpreted with Ag occupying site F' rather than site I (as in the annealed 0.6-ML system) because a polarization dependence of R, which was attributed to the effect of $\Delta_{Ag}(k)$, was observed for the 0.6-ML system [2.48±0.04 Å (90°), 2.46±0.04 Å (25°)], whereas for the 0.33-ML system it was not [2.48±0.05 Å for 90° and 25°]. The isotropic R was explained as a cancellation between the effects of $\Delta_{Ag}(k)$ and of ΔR. However, (i) Table V shows that the effect of ΔR for site F' exceeds that of $\Delta_{Ag}(k)$, (ii) Fig. 15 shows that the predicted effect of ΔR on the amplitude for site F' is unusually large and this was not reported, and (iii) the value of $R_1=2.34$ Å assumed for this site (see Table IV) is much shorter than the

sum of Ag-Si covalent radii, 2.51 A. A more likely explanation of the 0.33-ML data is that (i) Ag does occupy site F' but with a value of $R_1 \sim 2.5$ Å, (ii) the uncertainties in the measured $R(25°)$ and $R(90°)$ values obscure the actual small (~ 0.01 Å) anisotropy due to $\Delta_{Ag}(k)$, and (iii) the contributions from the second-neighbor Si shell at $R_2 \sim 2.95$ Å (see Table IV) are negligible (i.e., $a(\theta)$ is $\ll 1$) due to their larger distance and the probable static disorder from the as-deposited Ag. A comparison of SEXAFS amplitudes from the 0.6- and 0.33-ML data should clarify this point.